

arXiv:0709.1775 [hep-ph]  
JLAB-THY-07-718

# A Review of Target Mass Corrections<sup>‡</sup>

Ingo Schienbein,<sup>a,b</sup> Voica A. Radescu,<sup>c</sup> G.P. Zeller,<sup>d</sup>  
M. Eric Christy,<sup>e</sup> C.E. Keppel,<sup>e,f</sup> Kevin S. McFarland,<sup>g</sup>  
W. Melnitchouk,<sup>f</sup> Fredrick I. Olness,<sup>b,§</sup> Mary Hall Reno,<sup>h,||</sup>  
Fernando Steffens,<sup>i</sup> Ji-Young Yu,<sup>b</sup>

<sup>a</sup>Laboratoire de Physique Subatomique & Cosmologie, F-38026 Grenoble, France

<sup>b</sup>Southern Methodist University, Dept. of Physics, Dallas, TX 75275, USA

<sup>c</sup>Deutsches Elektronen Synchrotron, Notkestrasse 85, D-22603 Hamburg, Germany

<sup>d</sup>Los Alamos National Laboratory, Los Alamos, NM 87545, USA

<sup>e</sup>Hampton University, Dept. of Physics, Hampton, VA 23668, USA

<sup>f</sup>Jefferson Lab, Newport News, VA 23606, USA

<sup>g</sup>University of Rochester, Dept. of Physics & Astronomy, Rochester, NY 14627-0171, USA

<sup>h</sup>University of Iowa, Dept. of Physics and Astronomy, Iowa City, IA 52242, USA

<sup>i</sup>Mackenzie Presbiteriana Universidade, 01302-907, Sao Paulo, SP, Brazil

**Abstract.** With recent advances in the precision of inclusive lepton–nuclear scattering experiments, it has become apparent that comparable improvements are needed in the accuracy of the theoretical analysis tools. In particular, when extracting parton distribution functions in the large- $x$  region, it is crucial to correct the data for effects associated with the nonzero mass of the target. We present here a comprehensive review of these target mass corrections (TMC) to structure functions data, summarizing the relevant formulas for TMCs in electromagnetic and weak processes. We include a full analysis of both hadronic and partonic masses, and trace how these effects appear in the operator product expansion and the factorized parton model formalism, as well as their limitations when applied to data in the  $x \rightarrow 1$  limit. We evaluate the numerical effects of TMCs on various structure functions, and compare fits to data with and without these corrections.

<sup>‡</sup> J. Phys. G: Nucl. Part. Phys. 35 (2008) 053101

<sup>§</sup> Corresponding author e-mail: olness@smu.edu

<sup>||</sup> Corresponding author e-mail: mary-hall-reno@uiowa.edu

<i>CONTENTS</i>	2
-----------------	---

## Contents

<b>1 Introduction</b>	<b>3</b>
<b>2 Structure Functions and the Operator Product Expansion</b>	<b>4</b>
2.1 Overview of Structure Functions and the OPE . . . . .	4
2.2 Master Equations . . . . .	9
2.3 Nachtmann Moments . . . . .	10
<b>3 Relation of the OPE to the Parton Model</b>	<b>12</b>
<b>4 Corrections for Finite Hadron and Quark Masses</b>	<b>14</b>
4.1 Multiple Mass Scales in Neutrino DIS . . . . .	15
4.2 Relation to TMC Structure Functions . . . . .	16
<b>5 Threshold Effects and the <math>x \rightarrow 1</math> Limit</b>	<b>17</b>
<b>6 Quantitative Effects of Target Mass Corrections</b>	<b>21</b>
6.1 TMC Effects in the Massless Quark Limit . . . . .	21
6.2 Non-leading Terms in the Master Equations . . . . .	22
6.3 TMC Effects in NuTeV Structure Functions . . . . .	25
6.4 Unfolding Target Mass Effects From Structure Function Data . . . . .	25
6.5 Longitudinal Structure Function . . . . .	29
<b>7 Conclusions</b>	<b>31</b>
<b>Appendix A</b>	
<b>Kinematics and Fundamental Relations</b>	<b>32</b>
Appendix A.1	
Notation . . . . .	32
Appendix A.2	
Generalized Nachtmann Variable . . . . .	33
<b>Appendix B</b>	
<b>Charm Mass Dependence in <math>h_2</math> and <math>g_2</math></b>	<b>34</b>
<b>Appendix C</b>	
<b>Comparisons with the Literature</b>	<b>35</b>
Appendix C.1	
Comparisons with Georgi & Politzer . . . . .	35
Appendix C.2	
Comparisons with Barbieri, Ellis, Gaillard, & Ross . . . . .	36
Appendix C.3	
Comparisons with Kretzer & Reno . . . . .	37

## 1. Introduction

The scattering of electrons on hadronic targets has historically played an essential role in our understanding of the proton as a composite particle made up of partons: quarks and gluons [1–4]. Presently, data from electron and neutrino scattering at large momentum transfers, that is, deeply inelastic scattering (DIS), are used to determine the parton distribution functions (PDFs) which characterize the substructure of hadrons [5–10]. At lower energies, the resonant components of hadronic structure, and the duality between hadronic and partonic descriptions of interactions, continue to be explored [11, 12].

As the precision of the recent lepton–hadron scattering data has improved, it is vital for the theoretical analysis to keep pace. For example, the calculation of the Wilson coefficients has progressed to encompass next-to-leading order (NLO) quantum chromodynamics (QCD) and beyond [13–22]. It is important, therefore, to consider all sources of corrections which may contribute at a comparable magnitude, such as electroweak radiative corrections [23, 24], quark mass effects [25–32], and target mass corrections [33–40]. In this review, we will focus on the problem of target mass corrections (TMCs), which formally are subleading  $1/Q^2$  corrections to leading twist structure functions, where  $Q^2$  is the squared four-momentum transfer to the hadron.

Understanding TMCs is important for several reasons. Their effects are most pronounced at large  $x$  and moderate  $Q^2$ , which coincides with the region where parton distribution functions (PDFs) are not very well determined. A reliable extraction of PDFs here therefore demands an accurate description of the TMCs. Furthermore, a reliable interpretation of data on multiparton correlations at low momentum transfer depends on the proper accounting of TMCs. While target mass corrections have a long history, implementing these has not been entirely straightforward, as there exist a number of conventions, prescriptions, and potential scheme choices which can lead to differences in the final numerical results.

The target mass corrections to electroweak structure functions were first determined by Georgi and Politzer in 1976 [34] within the operator product expansion (OPE) at the leading order of QCD. In the same year Barbieri et al. [35, 36] rederived the mass corrections to scaling in DIS, including effects arising from non-zero quark masses. These same corrections were later derived from a parton model approach by Ellis, Furmanski and Petronzio [37, 38]. Beyond leading order, the NLO QCD corrections to the target mass corrected structure functions were derived by De Rújula, Georgi and Politzer [39]. Recently, Kretzer and Reno [41, 42] reevaluated the TMCs for charged current (CC) and neutral current (NC)  $\mu$ - and  $\tau$ - neutrino DIS, including NLO QCD corrections.

There is a number of theoretical ingredients necessary to derive the TMCs to hadronic structure functions in lepton–hadron scattering in the context of the OPE, in order to relate them to the quark-parton model (QPM). The OPE method makes use of basic fundamental symmetries to relate the cross section to a reduced matrix element; as such, the OPE takes the hadron mass fully into account. In order to relate the reduced matrix elements to quantities which can be computed in the QPM, one then

inherits the associated limitations. For example, the QPM describes the interaction as involving the scattering from a single, free parton (the leading twist contribution, see Sec. 2). Multi-parton correlations, formally higher twist, are discarded. Additionally, the QPM also imposes collinear kinematics on the parton involved in the interaction. The potential for the parton momentum to have a non-zero component transverse to the hadron momentum vector is neglected. This effect can omit mass contributions and introduce ambiguities if not addressed carefully.

When using the QPM approach, the target mass corrections are taken into account in the following places:

- in relating the parton fraction of the hadron’s light-cone momentum (called the Nachtmann variable) to the Bjorken scaling variable  $x = Q^2/2M\nu$ , where  $M$  is the hadron mass and  $\nu$  the energy transfer;
- in the mixing between the partonic and hadronic structure functions;
- in a collinear expansion, where the TMCs appear from the  $p_T$  effects .

In the limit of negligible target mass relative to  $Q^2$ , the Nachtmann variable reduces to Bjorken- $x$ . The QPM approach including TMCs has further limitations in the limit as  $x \rightarrow 1$ . A “threshold problem” arises when trying to enforce that the structure functions vanish in kinematically forbidden regions.

In the next section, we review structure functions and the OPE approach. We show the OPE results for the structure functions. Section 3 discusses the relation of the OPE to the parton model. We illustrate the formalism with the example of neutrino charged current scattering in Section 4. Section 5 describes the  $x \rightarrow 1$  problem and recent attempts to resolve this theoretical issue. Finally, in Section 6, we make some numerical comparisons using structure functions with and without target mass corrections. Our conclusions are summarized in Section 7. Three appendices detail the notation used in this review, the inclusion of charm mass corrections in neutrino charged current scattering, and a comparison of notation and results with Refs. [34, 35, 40] and [42].

## 2. Structure Functions and the Operator Product Expansion

In this section we present an overview of the formalism for deep inelastic scattering (DIS). Using the framework of the operator product expansion (OPE), we outline the derivation of the leading electromagnetic and weak structure functions at finite  $Q^2$ , including corrections from the non-zero target nucleon mass. We summarize these in a set of so-called “master equations”. Finally, we present an alternative but equivalent formulation of target mass correction (TMC) effects through the Nachtmann moments, and contrast this with the formulation in terms of Cornwall–Norton moments.

### 2.1. Overview of Structure Functions and the OPE

The basic lepton–nucleon inelastic scattering process,  $\ell(k) + N(P) \rightarrow \ell'(k') + X(P_X)$ , is shown schematically in Fig. 1, where  $k(k')$  is the initial (final) lepton four-momentum,

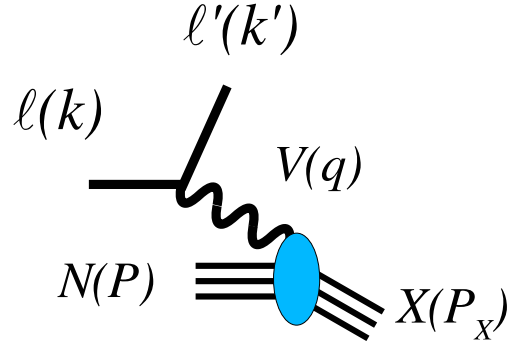


**Figure 1.** The basic deep inelastic lepton–nucleon scattering process,  $\ell(k) + N(P) \rightarrow \ell'(k') + X(P_X)$ .

$P$  is the target nucleon momentum, and  $P_X$  is the momentum of the final hadronic state  $X$ . We define  $q = k - k'$  to be the four-momentum transferred from the lepton to the nucleon, with  $Q^2 \equiv -q^2$ . The energies of the initial and final leptons are denoted by  $E$  and  $E'$ , respectively. Our notation reserves  $M$  for the target nucleon mass,  $P^2 = M^2$ , and the invariant mass squared of the final hadronic state is given by  $P_X^2 = W^2 = (P + q)^2 = M^2 + 2P \cdot q - Q^2$  (see also Appendix A).

For electromagnetic or weak neutral current (NC) scattering, the vector boson ( $V$ )–nucleon subprocess is  $V(q) + N(P) \rightarrow X(P_X)$ , where  $V = \gamma, Z^0$ . The related charged current (CC) process, which is important in neutrino–hadron scattering,  $\nu(k) + N(p) \rightarrow \ell(k') + X(P_X)$ , where  $V = W^\pm$ , will be discussed in Sec. 3, where we discuss the correspondence with the parton model.

In addition to the virtuality of the exchanged boson,  $Q^2$ , inelastic scattering is also characterized by the Bjorken scaling variable  $x$ , where

$$x = \frac{Q^2}{2P \cdot q}. \quad (1)$$

In the massless target and quark limits (or equivalently in the  $Q^2 \rightarrow \infty$  limit),  $x$  is equivalent to the light-cone momentum fraction of the target carried by the interacting parton. In the target rest frame, the Bjorken variable can be written  $x = Q^2/2M\nu$ , where  $\nu = E - E'$  is the energy transferred to the hadronic system, and we define the inelasticity of the process by  $y = \nu/E$ . For convenience, we also introduce the variable  $r$  to denote a frequently appearing combination of factors:

$$r = \sqrt{1 + \frac{4x^2 M^2}{Q^2}} \equiv \sqrt{1 + \frac{Q^2}{\nu^2}}. \quad (2)$$

At finite  $Q^2$ , the effects of the target and quark masses modify the identification of the Bjorken  $x$  variable with the light-cone momentum fraction. For massless quarks, the parton light-cone fraction is given by the Nachtmann variable  $\xi$  [33],

$$\xi = \frac{2x}{1 + \sqrt{1 + 4x^2 M^2 / Q^2}}. \quad (3)$$

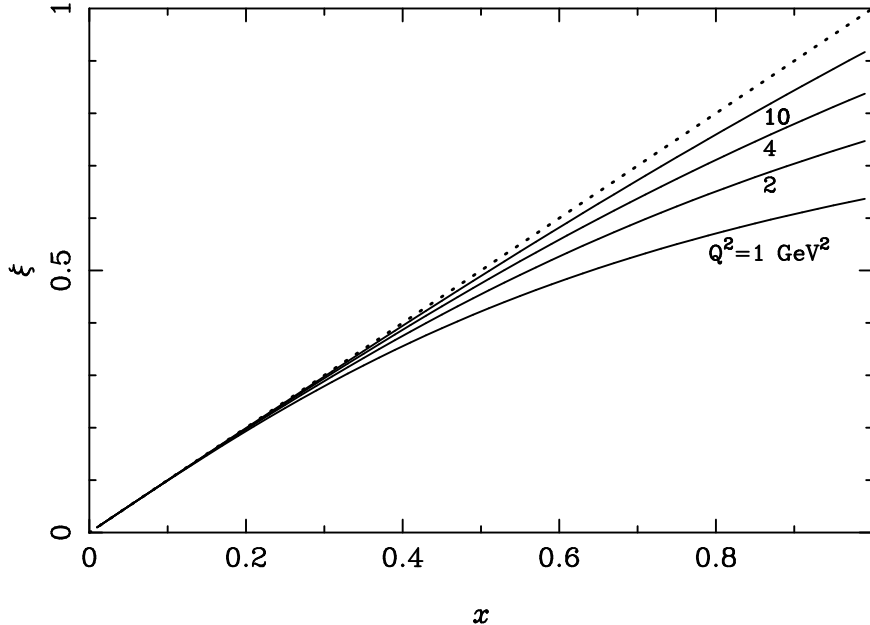


**Figure 2.** The Nachtmann variable  $\xi$  as a function of the Bjorken scaling variable  $x$ , for  $Q^2 = 1, 2, 4$  and  $10 \text{ GeV}^2$ . For reference, a dotted line is shown for the limiting case  $\xi = x$ .

At large values of  $Q^2$ ,  $\xi \sim x$ . As Fig. 2 shows, however, for  $Q^2$  less than a few times the target mass of  $\sim 1 \text{ GeV}$ ,  $\xi$  can deviate significantly from  $x$ , especially at large  $x$  values. The Nachtmann variable appears naturally in the OPE, as we outline below. The full details of the notation, including parton masses, appear in Appendix A.

We can write any generic inclusive lepton–nuclear scattering cross section as a combination of a hadronic tensor  $W_{\mu\nu}$  and a leptonic tensor  $L^{\mu\nu}$ :

$$d\sigma \sim W_{\mu\nu} L^{\mu\nu},$$

where the hadronic tensor is given in terms of a product of hadronic currents,<sup>¶</sup>

$$\begin{aligned} W_{\mu\nu} &\equiv \frac{1}{2\pi} \int d^4z e^{iq\cdot z} \langle N | [J_\mu(z), J_\nu(0)] | N \rangle \\ &= -g_{\mu\nu} W_1 + \frac{p_\mu p_\nu}{M^2} W_2 - i\epsilon_{\mu\nu\rho\sigma} \frac{p^\rho q^\sigma}{M^2} W_3 \\ &\quad + \frac{q_\mu q_\nu}{M^2} W_4 + \frac{p_\mu q_\nu + p_\nu q_\mu}{M^2} W_5. \end{aligned} \quad (4)$$

The structure functions  $W_i$  depend on  $x$  and  $Q^2$ , as well as the target mass  $M$ . The hadronic tensor can be related to the discontinuity of the virtual forward Compton scattering amplitude  $T_{\mu\nu}$  via

$$W_{\mu\nu} = \frac{1}{\pi} \text{disc } T_{\mu\nu}. \quad (5)$$

<sup>¶</sup> In this work, we will focus on the unpolarized results. For TMC effects on the polarized structure function see Refs. [43–45], and references therein.

The OPE allows one to expand the hadronic matrix element in the forward scattering amplitude in a complete set of local operators [46]:

$$\begin{aligned} T_{\mu\nu} &\equiv i \int d^4z e^{iq\cdot z} \langle N | T[J_\mu(z) J_\nu(0)] | N \rangle \\ &= \sum_{i,\tau,n} c_{\tau,\mu\nu}^{i,\mu_1 \dots \mu_n}(q) \langle N | O_{\mu_1 \dots \mu_n}^{i,\tau} | N \rangle , \end{aligned} \quad (6)$$

where the coefficient functions  $c_{\tau,\mu\nu}^{i,\mu_1 \dots \mu_n}(q)$  represent the hard scattering of the boson from the parton. Here  $\tau$  denotes the twist of the operator  $O$ , defined to be the mass dimension minus the spin of the operator, and  $i$  represents different operators with the same twist.

In the approximation of keeping only twist-2 operators,<sup>+</sup> the forward scattering amplitude is explicitly:

$$\begin{aligned} T^{\mu\nu} = & \sum_{k=1}^{\infty} \left( -g^{\mu\nu} q_{\mu_1} q_{\mu_2} C_1^{2k} + g_{\mu_1}^\mu g_{\mu_2}^\nu Q^2 C_2^{2k} - i\epsilon^{\mu\nu\alpha\beta} g_{\alpha\mu_1} q_\beta q_{\mu_2} C_3^{2k} \right. \\ & \left. + \frac{q^\mu q^\nu}{Q^2} q_{\mu_1} q_{\mu_2} C_4^{2k} + (g_{\mu_1}^\mu q^\nu q_{\mu_2} + g_{\mu_1}^\nu q^\mu q_{\mu_2}) C_5^{2k} \right) q_{\mu_3} \cdots q_{\mu_{2k}} \\ & \times \frac{2^{2k}}{Q^{4k}} A_{2k} \Pi^{\mu_1 \dots \mu_{2k}} , \end{aligned} \quad (7)$$

where  $A_{2k}$  is the reduced matrix element of the twist-2 operator of spin  $2k$ , and  $C_i^{2k}$  is the Wilson coefficient calculated using perturbative QCD. In Eq. (7),

$$\Pi^{\mu_1 \dots \mu_{2k}} = \sum_{j=0}^k (-1)^j \frac{(2k-j)!}{2^j (2k)!} \underbrace{\{g \dots g\}}_{j \text{ } g^{\mu_1 \dots \mu_m} s} \underbrace{\{p \dots p\}}_{(2k-2j) \text{ } p^{\mu_n \dots \mu_s}} (p^2)^j , \quad (8)$$

where  $\{g \dots g\}$   $\{p \dots p\}$  abbreviates a sum over  $(2k)!/[2^j j! (2k-2j)!]$  permutations of the indices.

The strategy in the calculation, as outlined by Georgi and Politzer [34], is to evaluate Eq. (7), picking off each of the coefficients in the expansion,

$$T_{\mu\nu} = -g_{\mu\nu} T_1 + \frac{p_\mu p_\nu}{M^2} T_2 - i\epsilon_{\mu\nu\rho\sigma} \frac{p^\rho q^\sigma}{M^2} T_3 + \frac{q_\mu q_\nu}{M^2} T_4 + \frac{p_\mu q_\nu + p_\nu q_\mu}{M^2} T_5 . \quad (9)$$

Finally, the structure functions  $W_i$  can be obtained from the imaginary parts of the amplitudes  $T_i$  using Eq. (5). In modern notation, the structure functions are denoted by  $F_i$  rather than  $W_i$ . To emphasize the inclusion of target mass corrections in the structure functions, we label  $F_i \rightarrow F_i^{\text{TMC}}$ , and note the correspondence

$$\begin{aligned} & \left\{ F_1, F_2, F_3, F_4, F_5 \right\}^{\text{TMC}} \\ &= \left\{ W_1, \frac{Q^2}{2xM^2} W_2, \frac{Q^2}{xM^2} W_3, \frac{Q^2}{2M^2} W_4, \frac{Q^2}{2xM^2} W_5 \right\} . \end{aligned} \quad (10)$$

In the following discussion, we focus on  $F_1^{\text{TMC}}$ ,  $F_2^{\text{TMC}}$  and  $F_3^{\text{TMC}}$ . The remaining two structure functions enter into the differential cross section suppressed by the lepton mass squared divided by  $ME$  [42], and can for most purposes be neglected.

<sup>+</sup> For a NLO calculation including an analysis of higher twist contributions see, for example, Refs. [47–49]

Using Eqs. (5) and (7), one can explicitly relate the Cornwall–Norton moments  $M_i^n(Q^2)$  of the  $F_i^{\text{TMC}}$  structure functions to sums of reduced matrix elements [34, 50]. For the  $F_2^{\text{TMC}}$  structure function, for example, one has:

$$\begin{aligned} M_2^n(Q^2) &= \int_0^1 dx x^{n-2} F_2^{\text{TMC}}(x, Q^2) \\ &= \sum_{j=0}^{\infty} \left( \frac{M^2}{Q^2} \right)^j \frac{(n+j)!}{j!(n-2)!} \frac{C_2^{n+2j} A_{n+2j}}{(n+2j)(n+2j-1)} . \end{aligned} \quad (11)$$

Defining  $F_i^{(0)}$  to be the massless nucleon limits of the structure functions  $F_i^{\text{TMC}}$ , we can relate the reduced matrix elements in Eq. (11) to the Cornwall–Norton moments of  $F_i^{(0)}$ :

$$C_2^{n+2j} A_{n+2j} \equiv \int_0^1 dy y^{n+2j-2} F_2^{(0)}(y) , \quad (12)$$

$$C_i^{n+2j} A_{n+2j} \equiv \int_0^1 dy y^{n+2j-1} F_i^{(0)}(y) , \quad i = 1, 3 . \quad (13)$$

In other words, the functions  $F_i^{\text{TMC}}$  contain target mass effects, whereas the  $F_i^{(0)}$  do not.

The Cornwall–Norton moments can be inverted to yield a set of target mass corrected structure functions derived from the operator product expansion:

$$F_1^{\text{TMC}}(x, Q^2) = \frac{x}{\xi r} F_1^{(0)}(\xi) - \frac{M^2 x^2}{Q^2} \frac{\partial}{\partial x} \left\{ \frac{1+r}{r} g_2(\xi) \right\} , \quad (14)$$

$$F_2^{\text{TMC}}(x, Q^2) = x^2 \frac{\partial^2}{\partial x^2} \left\{ \frac{(1+r)^2}{4r} g_2(\xi) \right\} , \quad (15)$$

$$F_3^{\text{TMC}}(x, Q^2) = -x \frac{\partial}{\partial x} \left( \frac{1+r}{2r} h_3(\xi) \right) . \quad (16)$$

The  $F_2^{\text{TMC}}$ -expression comes from Eq. (4.17) of Ref. [34], and  $F_1^{\text{TMC}}$  and  $F_3^{\text{TMC}}$  follow in the same manner. The functions  $g_2$  and  $h_3$  along with two more auxiliary functions  $h_{1,2}$ , which will be needed below, are given by [42]:

$$h_1(\xi, Q^2) = \int_\xi^1 du \frac{2F_1^{(0)}(u, Q^2)}{u} , \quad (17)$$

$$h_2(\xi, Q^2) = \int_\xi^1 du \frac{F_2^{(0)}(u, Q^2)}{u^2} , \quad (18)$$

$$h_3(\xi, Q^2) = \int_\xi^1 du \frac{F_3^{(0)}(u, Q^2)}{u} , \quad (19)$$

$$g_2(\xi, Q^2) = \int_\xi^1 du h_2(u, Q^2) = \int_\xi^1 du \int_u^1 dv \frac{F_2^{(0)}(v, Q^2)}{v^2} \quad (20)$$

$$= \int_\xi^1 dv \int_\xi^{u_{\max}=v} du \frac{F_2^{(0)}(v, Q^2)}{v^2} = \int_\xi^1 dv (v - \xi) \frac{F_2^{(0)}(v, Q^2)}{v^2} .$$

Evaluating the derivatives in Eqs. (14)–(16) yields our final set of “master equations” for the target mass corrected DIS structure functions, which we discuss next.

## 2.2. Master Equations

Combining the results in the previous section, the full, target mass corrected structure functions can be related to the massless limit functions by the following “master formula”, using the notation of Kretzer & Reno (see Eq. (3.17) of Ref. [42], with their  $\rho \rightarrow r$ ):

$$F_j^{\text{TMC}}(x, Q^2) = \sum_{i=1}^5 A_j^i F_i^{(0)}(\xi, Q^2) + B_j^i h_i(\xi, Q^2) + C_j g_2(\xi, Q^2), \quad j = 1 - 5, \quad (21)$$

where  $\xi$  is the Nachtmann scaling variable from Eq. (3) [33]. Inserting the coefficients  $A_j^i$ ,  $B_j^i$ ,  $C_j$  given in Tables I, II and III of Ref. [42], one finds for the first three structure functions:

$$F_1^{\text{TMC}}(x, Q^2) = \frac{x}{\xi r} F_1^{(0)}(\xi, Q^2) + \frac{M^2 x^2}{Q^2 r^2} h_2(\xi, Q^2) + \frac{2M^4 x^3}{Q^4 r^3} g_2(\xi, Q^2), \quad (22)$$

$$F_2^{\text{TMC}}(x, Q^2) = \frac{x^2}{\xi^2 r^3} F_2^{(0)}(\xi, Q^2) + \frac{6M^2 x^3}{Q^2 r^4} h_2(\xi, Q^2) + \frac{12M^4 x^4}{Q^4 r^5} g_2(\xi, Q^2), \quad (23)$$

$$F_3^{\text{TMC}}(x, Q^2) = \frac{x}{\xi r^2} F_3^{(0)}(\xi, Q^2) + \frac{2M^2 x^2}{Q^2 r^3} h_3(\xi, Q^2) + 0, \quad (24)$$

with the functions  $h_i(\xi, Q^2)$  and  $g_2(\xi, Q^2)$  given in Eqs. (17)–(20). The  $F_j^{(0)}$  are the structure functions  $F_j^{\text{TMC}}$  in the limit  $M \rightarrow 0$ :

$$F_j^{(0)}(\xi, Q^2) \equiv \left( \lim_{M \rightarrow 0} F_j^{\text{TMC}}(x, Q^2) \right) \Big|_{x=\xi}. \quad (25)$$

Note that since  $\xi$  depends on  $x$  and  $M$ ,  $F_j^{(0)}(\xi, Q^2) \neq \lim_{M \rightarrow 0} F_j^{\text{TMC}}(\xi, Q^2)$ , which has been the source of some confusion in the literature. Parton model representations of  $F_j^{(0)}$  will be shown in Sec. 4.

We emphasize that the functions  $F_i^{\text{TMC}} = F_i^{\text{TMC}}(x, Q^2)$ , and not  $F_i^{\text{TMC}} = F_i^{\text{TMC}}(\xi, Q^2)$ , so that  $(x, Q^2)$  is the correct point in phase space. While on the surface it may appear strange to have the left-hand-side of Eq. (21) be a function of  $x$  and the right-hand-side a function of  $\xi$ , this arises quite naturally in the calculation. Specifically, evaluating the final state momentum conservation constraint, we can write (schematically)  $\delta^4(q+P-P_X) \sim \delta(x-\xi)$ , and thus  $F_i^{\text{TMC}}(x, Q^2) \sim F_i^{(0)}(x, Q^2) \delta(x-\xi) \sim F_i^{(0)}(\xi, Q^2)$ . Note that it would be incorrect to write  $F_i^{\text{TMC}}(\xi, Q^2) \sim F_i^{(0)}(\xi, Q^2)$ . All structure functions and PDFs depend on  $Q^2$ ; we sometimes suppress this dependence for ease of notation.

Another feature of Eq. (21) is that  $h_2$  and  $g_2$  appear in the formulas for both  $F_1^{\text{TMC}}$  and  $F_2^{\text{TMC}}$ . This follows directly from the form of Eq. (7). For example, both the terms proportional to  $C_1^{2k}$  and to  $C_2^{2k}$  contribute to  $T_1$  (multiplying  $-g_{\mu\nu}$ ). The terms proportional to  $C_2^{2k}$  give rise to the second and third terms in Eq. (22).

The “master equation” (21) holds to any order in the strong coupling constant  $\alpha_s$ , which implies that the coefficients  $A_j^i$ ,  $B_j^i$  and  $C_j$  and the variable  $\xi$  are independent of

the order (LO, NLO, NNLO, ...) to which the structure functions  $F_i^{(0)}$  are considered. In addition, Eq. (21) does not assume or imply any Callan–Gross relation. Specifically, one can compute the longitudinal structure function according to:

$$\begin{aligned} F_L^{\text{TMC}}(x, Q^2) &= r^2 F_2^{\text{TMC}}(x, Q^2) - 2x F_1^{\text{TMC}}(x, Q^2) \\ &= \frac{x^2}{\xi^2 r} [F_2^{(0)}(\xi) - 2\xi F_1^{(0)}(\xi)] + \frac{4M^2 x^3}{Q^2 r^2} h_2(\xi) + \frac{8M^4 x^4}{Q^4 r^3} g_2(\xi) \\ &= \frac{x^2}{\xi^2 r} F_L^{(0)}(\xi) + \frac{4M^2 x^3}{Q^2 r^2} h_2(\xi) + \frac{8M^4 x^4}{Q^4 r^3} g_2(\xi). \end{aligned} \quad (26)$$

This general result gives a non-zero  $F_L^{\text{TMC}}$ , and thus violates the Callan–Gross relation. The leading term ( $\propto F_L^{(0)}$ ) is non-zero for finite quark masses, and the sub-leading terms ( $\propto h_2, g_2$ ) contribute for finite hadron mass  $M$ .

Final state quark mass effects are taken into account by the parton model structure functions  $F_i^{(0)}$ , and the general form of the master equation is unaltered. In other words, the  $\{A_j^i, B_j^i, C_j^i\}$  coefficients and the Nachtmann variable  $\xi$  in Eq. (21) will depend only on the hadronic mass and will *not* receive corrections due to final state quark masses. We illustrate this feature for the case of neutrino production of charm quarks in Sec. 4, and find agreement with results in the literature (*cf.* Appendix C). In particular, the proper slow-rescaling variables (which depend on the quark masses) automatically appear as arguments of the parton distribution functions in a natural manner (*cf.* Appendix A). For the general case of non-vanishing initial and final state quark masses we *assume* the same pattern holds true—the quark masses appear within the  $F_i^{(0)}$  and the form of the master equation remains unchanged; this is a consequence of factorization. This ensures the correct massive parton model expressions are, by construction, recovered in the  $M \rightarrow 0$  limit; a necessary condition for any formalism which includes target mass effects. The modular structure of the master equation renders computations of target mass corrections simple and transparent once the parton model expressions for the  $F_i^{(0)}$  (with or without quark masses, in leading or higher order) are given.

### 2.3. Nachtmann Moments

An alternative, but closely related, formulation of the TMCs is in terms of *Nachtmann moments*. Nachtmann [33] showed that one could arrange the OPE so as to ensure that at a given order in  $1/Q^2$  only operators of a given twist would appear. The Nachtmann moments  $\mu_i^n$  of structure functions  $F_i^{\text{TMC}}$  ( $i = 1, 2, 3$ ) are constructed from operators of definite spin. This means that from the infinite set of operators of twist-two and different spin contained in the trace terms of the OPE, only the operators of spin  $n$  contribute for the  $n - 2$  Nachtmann moment of the structure function. This is contrasted with the Cornwall–Norton moments in which different spin operators contribute to the twist-two moment. The Nachtmann moments are defined to factor out the target mass dependence of the structure functions in a way such that its (Cornwall–Norton) moments would equal the moments of the corresponding parton distributions.

For the  $F_2^{\text{TMC}}$  structure function for example, the Nachtmann moment is constructed so that it depends only on the reduced matrix element  $A_n$  (and Wilson coefficient  $C_i^n$ ) on the right-hand-side of Eq. (11), in contrast to the infinite series of  $(M^2/Q^2)^j$  terms in Eq. (11) for the Cornwall–Norton moment. In effect, the subleading  $(M^2/Q^2)^j$  terms with  $j \geq 1$  are absorbed in the redefined moment on the left-hand-side of Eq. (11), so that only the first term with  $j = 0$  contributes to the Nachtmann moment.

Specifically, the Nachtmann moment of the  $F_2$  structure function is given by:

$$\mu_2^n(Q^2) = \int_0^1 dx \frac{\xi^{n+1}}{x^3} \left[ \frac{3 + 3(n+1)r + n(n+2)r^2}{(n+2)(n+3)} \right] F_2^{\text{TMC}}(x, Q^2), \quad (27)$$

where again we use  $r = \sqrt{1 + 4x^2 M^2/Q^2}$ . One can also express the Nachtmann moment as an integral over the Nachtmann variable  $\xi$ ,

$$\begin{aligned} \mu_2^n(Q^2) &= \int_0^{\xi_0} d\xi \xi^{n-2} \frac{(1 + \xi^2 M^2/Q^2)^3}{1 - \xi^2 M^2/Q^2} \left[ 1 - \frac{3(r-1)}{r^2(n+2)} - \frac{3(r-1)^2}{r^2(n+3)} \right] \\ &\times F_2^{\text{TMC}}(x, Q^2) |_{x=\xi/(1-M^2\xi^2/Q^2)}, \end{aligned} \quad (28)$$

with  $F_2^{\text{TMC}}(x, Q^2)$  given by Eq. (23), and  $\xi_0 = \xi(x=1) = 2/(1 + \sqrt{1 + 4M^2/Q^2})$ .

Similarly, for the longitudinal Nachtmann moments (or equivalently for the  $F_1^{\text{TMC}}$  structure function, defined in terms of  $F_2^{\text{TMC}}$  and  $F_L^{\text{TMC}}$ ), one has [33]:

$$\begin{aligned} \mu_L^n(Q^2) &= \int_0^1 dx \frac{\xi^{n+1}}{x^3} \left\{ F_L^{\text{TMC}}(x, Q^2) \right. \\ &\left. + \frac{4M^2 x^2}{Q^2} \frac{(n+1)\xi/x - 2(n+2)}{(n+2)(n+3)} F_2^{\text{TMC}}(x, Q^2) \right\}. \end{aligned} \quad (29)$$

Note that while in the  $Q^2 \rightarrow \infty$  limit  $\mu_L^n(Q^2)$  approaches the Cornwall–Norton moment of  $F_L^{\text{TMC}}$ , at finite  $Q^2$  both  $F_L^{\text{TMC}}$  and  $F_2^{\text{TMC}}$  contribute.

The Nachtmann moment  $\mu_2^n(Q^2)$  and Cornwall–Norton moment  $M_2^n(Q^2)$  can be related by expanding the moments in powers of  $1/Q^2$ . Expanding  $\mu_2^n$  to  $\mathcal{O}(1/Q^6)$ , one has:

$$\begin{aligned} \mu_2^n(Q^2) &= M_2^n(Q^2) - \frac{n(n-1)}{n+2} \frac{M^2}{Q^2} M_2^{n+2}(Q^2) \\ &+ \frac{n(n^2-1)}{2(n+3)} \frac{M^4}{Q^4} M_2^{n+4}(Q^2) - \frac{n(n^2-1)}{6} \frac{M^6}{Q^6} M_2^{n+6} + \dots, \end{aligned} \quad (30)$$

which illustrates the mixing between the lower and higher Cornwall–Norton moments.

In Fig. 3 we compare the  $n = 2$  Nachtmann moment  $\mu_2^{n=2}$  of the target mass corrected proton  $F_2^{\text{TMC}}$  structure function (solid curve) with the Cornwall–Norton moment  $M_2^{n=2}$  (dotted curve) of the same structure function in the massless target limit,  $F_2^{(0)}$  (note the expanded vertical scale!). While the two moments agree well at large  $Q^2$ , a clear deviation from equality is seen for  $Q^2 \lesssim 2 \text{ GeV}^2$ . Part of this discrepancy may be attributed to the behavior of the target mass corrected structure function in the  $x \rightarrow 1$  limit, as we discuss in detail in Sec. 5.

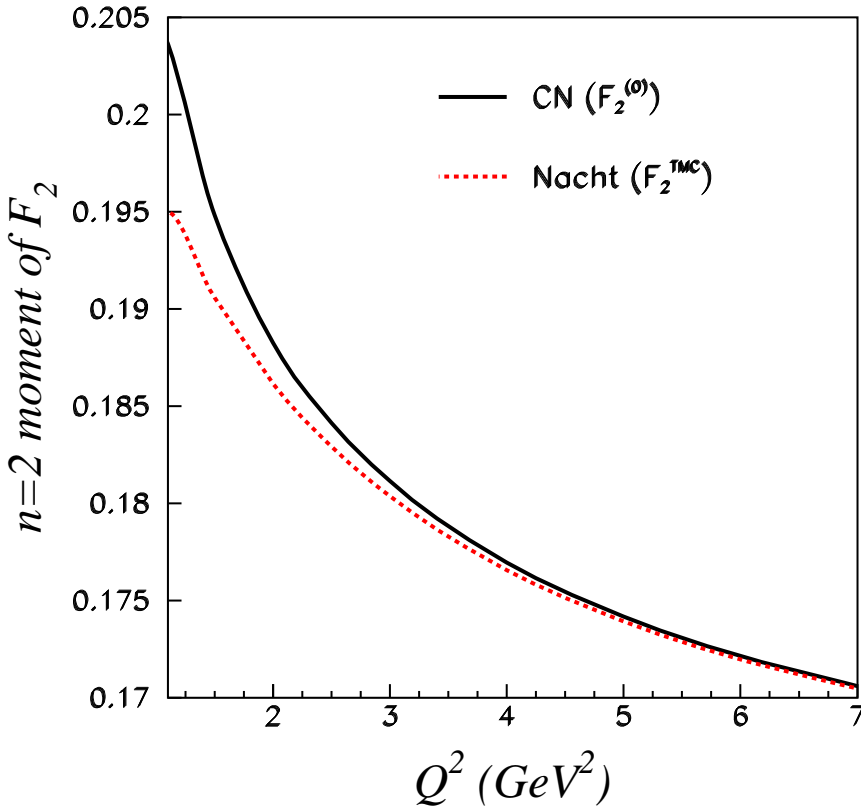


**Figure 3.** Comparison of the  $n = 2$  Cornwall–Norton moment of the proton  $F_2^{(0)}$  structure function (solid), with the Nachtmann moment of the target mass corrected  $F_2^{\text{TMC}}$  (dotted), calculated from  $F_2^{(0)}$  using Eq. (21).

### 3. Relation of the OPE to the Parton Model

In the previous section we used the OPE to relate the inclusive lepton–nuclear scattering cross section to the structure functions  $F_i^{(0)}$  of Eq. (21). While these relations are quite general, they are of no utility unless we can relate them to calculable quantities. Up to this point we have not invoked the parton model and its associated assumptions; the only ingredient has been the OPE, which only makes use of fundamental symmetries. In this section we briefly discuss the relation of the leading twist OPE treatment of inclusive lepton–nuclear scattering with the parton model. We also comment on the importance of TMCs in testing the validity of leading twist descriptions of data, or alternatively, extracting higher twist contributions.

The leading,  $j = 0$ , term in Eq. (8) reduces the target mass corrected structure function  $F_i^{\text{TMC}}$  to the massless limit function  $F_i^{(0)}$ , which can be expressed in terms of parton distributions in the parton model. The  $j > 0$  terms in Eq. (8) resum the target mass corrections. The explicit form of the structure functions  $F_i^{(0)}$  depends on

the interaction. For  $F_1^{(0)}$ , for example, the  $j = 0$  term in Eq. (13) can be schematically written (neglecting quark electroweak charges) as:

$$C_1^n \cdot A_n = \int_0^1 dx x^{n-1} F_1^{(0)}(x, Q^2) \quad (31)$$

$$= \int_0^1 dz z^{n-1} \sigma(z, Q^2, \mu^2) \cdot \int_0^1 dy y^{n-1} f(y, \mu^2) \quad (32)$$

$$= \int_0^1 dx x^{n-1} \int_x^1 \frac{dy}{y} \sigma\left(\frac{x}{y}, Q^2, \mu^2\right) f(y, \mu^2), \quad (33)$$

where  $f$  is the parton distribution function, defined at a scale  $\mu$ , and  $\sigma$  is the boson–parton scattering cross section. The first factor in the product  $C_1^n \cdot A_n$  above is the process-dependent Wilson coefficient, while the second is the moment of the parton distribution  $f$ . At leading order in QCD perturbation theory, the parton cross section  $\sigma(z, Q^2, \mu^2) \sim \delta(1 - z)$ , multiplied by numerical factors that account for the process (such as  $e_f^2/2$  for electromagnetic scattering with a parton of electric charge  $e_f$ ). QCD corrections introduce a  $Q^2$  dependence to  $\sigma$  and therefore to  $C_i^n$ . Both  $C_i^n$  and  $A^n$  depend on  $\mu^2$  in such a way that the product is  $\mu^2$  independent.

As remarked above, Eq. (21) is valid at leading twist, and to all orders in  $\alpha_s$ . The inclusion of higher orders in  $F_i^{(0)}$  is standard in the leading twist approximation. This involves evaluating the perturbative QCD corrections to  $Vq \rightarrow q$  and associated gluon processes. The NLO corrections have been known for some time [13–16, 27], and the NNLO corrections have also been evaluated [17–19, 21, 22, 51].

In addition to the perturbative corrections, moments of structure functions in the OPE receive  $1/Q^2$  power corrections, which are suppressed at large  $Q^2$ , but may be significant at lower  $Q^2$ . The size of these corrections is determined by matrix elements of local operators which have twist greater than 2, denoted “dynamical higher twist”. Since one of the motivations for studying TMCs is to more reliably extract leading twist parton distributions from structure function data, it is necessary to ensure that TMCs are properly taken into account so as to reveal genuine effects associated with dynamical higher twists. Of course, the TMCs themselves enter as  $1/Q^2$  corrections, despite formally being of leading twist, so in practice it is crucial to remove from the data TMC effects which could otherwise resemble higher twists.

The general expansion for the moments of structure functions in QCD is then one which involves an expansion in powers of  $1/Q^2$ , each term of which has an associated perturbative  $\alpha_s$  expansion, in addition to the  $(M^2/Q^2)^j$  TMC expansion as in Eq. (11). For the above example of the  $F_1$  structure function, the general OPE expansion in the  $M \rightarrow 0$  limit can be written [46]:

$$\int_0^1 dx x^{n-1} F_1^{(0)}(x, Q^2) = C_1^n(Q^2) A_n + \sum_{i=1}^{\infty} C_1^{n,i}(Q^2) \left(\frac{n M_0^2}{Q^2}\right)^i B_{n,i}, \quad (34)$$

where the first (twist-two) term corresponds to that in Eq. (31), and the higher twist coefficients  $B_{n,i}$  are of the same order as  $A_n$ , with  $M_0$  some typical hadronic mass scale.

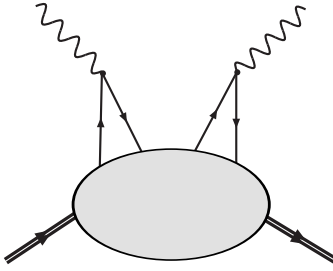


**Figure 4.** An example of a higher twist diagram, involving a four-quark operator, contributing to the term  $B_{n,i}$  in Eq. (34).

Several analyses of low  $Q^2$  data have been made which include both leading and higher twist contributions, although the practical difficulty in disentangling  $1/Q^2$  from even higher order corrections means that usually terms only up to twist 4 are considered.

Although in the context of parton distribution analyses higher twists are seen as unwelcome complications, the study of higher twists is also important in its own right. Because the higher twist operators necessarily involve several quark or quark and gluon fields, their matrix elements can provide insight into nonperturbative, multi-parton correlations in the nucleon, and possibly even on the long distance partonic interactions associated with confinement. For example, twist-4 corrections to the  $F_2$  structure function involve the so-called “cat’s ears” diagrams schematically shown in Fig. 4, which represent flavor non-diagonal transitions between the incoming and outgoing photons in the Compton scattering process [52]. Differences in their magnitude in the proton and neutron can reveal the mechanism responsible for the phenomenon of Bloom–Gilman duality in structure functions [12]. For spin dependent structure functions, certain twist-3 and twist-4 matrix elements can be related to color polarizabilities of the nucleon, which describe how the color electric and magnetic gluon fields respond to the spin of the nucleon [53–56]. Before we can begin to unravel these effects, it is essential that the kinematical TMCs are properly removed from the data.

Having outlined the formalism, in the next section we display explicit expressions for  $F_i^{(0)}$  for leading order QCD at leading twist for neutrino–proton scattering. We focus on this process because of the subtleties associated with charm production by massless quarks. Next-to-leading order expressions for the structure functions  $F_i^{(0)}$  in a fixed flavor number scheme with three active flavors (3-FFNS) can be found in Ref. [41].

#### 4. Corrections for Finite Hadron and Quark Masses

To illustrate how the OPE–parton model formalism is implemented in the case of a quark mass scale  $m_j$  in the final state (in addition to the target mass scale  $M$ ), we consider the case of neutrino inclusive lepton–nuclear scattering for 3 light  $\{u, d, s\}$  flavors and one heavy  $\{c\}$  flavor. The reaction takes place via the process  $\nu_\mu N \rightarrow \mu^- X$  (or  $\bar{\nu}_\mu N \rightarrow \mu^+ X$ ), *cf.* Fig. 5. In this example we will focus on the leading order only,

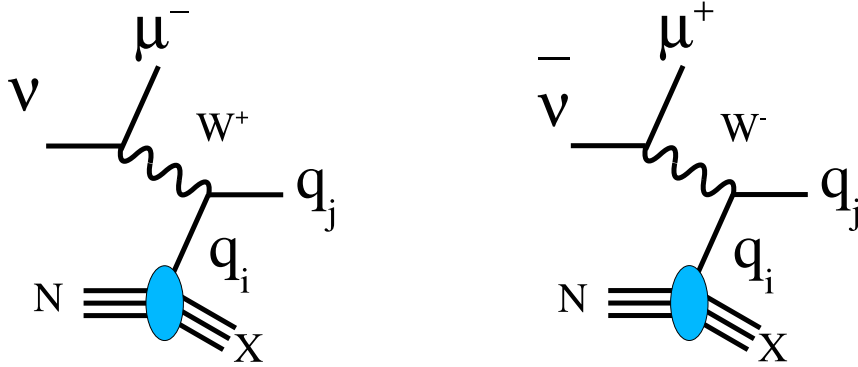


**Figure 5.** The basic Feynman diagrams for the DIS process for neutrinos,  $\nu N \rightarrow \mu^- X$  (left diagram) and anti-neutrinos  $\bar{\nu} N \rightarrow \mu^+ X$  (right diagram).

so we can separately observe how both  $M$  and  $m_j = m_c$  enter; once the pattern is developed here, the generalization to multiple quark masses ( $m_i, m_j$ ) will be outlined in Appendix A.

#### 4.1. Multiple Mass Scales in Neutrino DIS

To illustrate how the quark and hadron masses enter into the structure functions, we separate the  $M \rightarrow 0$  limit structure functions into contributions with a light ( $l$ ) and a heavy quark ( $c$ ) in the final state. For neutrino scattering, we thus have:

$$F_i^{\nu,(0)}(\xi, Q^2) = F_{i,l}^{\nu,(0)}(\xi, Q^2) + F_{i,c}^{\nu,(0)}(\xi, Q^2) . \quad (35)$$

For neutrino DIS with a light quark in the final state (*i.e.*, no charm), the structure functions for a 3-flavor number scheme are given by:

$$F_{1,l}^{\nu,(0)}(\xi, Q^2) = d(\xi)|V_{ud}|^2 + s(\xi)|V_{us}|^2 + \bar{u}(\xi)(|V_{ud}|^2 + |V_{us}|^2) , \quad (36)$$

$$F_{2,l}^{\nu,(0)}(\xi, Q^2) = 2\xi \left[ d(\xi)|V_{ud}|^2 + s(\xi)|V_{us}|^2 + \bar{u}(\xi)(|V_{ud}|^2 + |V_{us}|^2) \right] , \quad (37)$$

$$F_{3,l}^{\nu,(0)}(\xi, Q^2) = 2 \left[ d(\xi)|V_{ud}|^2 + s(\xi)|V_{us}|^2 - \bar{u}(\xi)(|V_{ud}|^2 + |V_{us}|^2) \right] , \quad (38)$$

where  $V_{ij}$  are the CKM matrix elements, and the  $Q^2$  dependence in the PDFs has been suppressed. For heavy quarks, the structure function contributions are:

$$F_{1,c}^{\nu,(0)}(\xi, Q^2) = d(\bar{\xi})|V_{cd}|^2 + s(\bar{\xi})|V_{cs}|^2 , \quad (39)$$

$$F_{2,c}^{\nu,(0)}(\xi, Q^2) = 2\bar{\xi} \left[ d(\bar{\xi})|V_{cd}|^2 + s(\bar{\xi})|V_{cs}|^2 \right] , \quad (40)$$

$$F_{3,c}^{\nu,(0)}(\xi, Q^2) = 2 \left[ d(\bar{\xi})|V_{cd}|^2 + s(\bar{\xi})|V_{cs}|^2 \right] . \quad (41)$$

For anti-neutrino structure functions  $F_i^{\bar{\nu},(0)}(\xi, Q^2)$ , the results are obtained by interchanging  $q \leftrightarrow \bar{q}$  in Eq. (35):

$$F_{1,2}^{\bar{\nu},(0)} = F_{1,2}^{\nu,(0)}[q \leftrightarrow \bar{q}] , \quad F_3^{\bar{\nu},(0)} = -F_3^{\nu,(0)}[q \leftrightarrow \bar{q}] , \quad q = u, d, s . \quad (42)$$

The variable  $\bar{\xi}$  in Eqs. (39)–(41) is the so-called slow rescaling variable, generalized to include both target and quark mass effects, and corresponds to the light-cone

fractional momentum of a massless quark which produces a charm quark. It is related to the Nachtmann scaling variable  $\xi$  by  $\bar{\xi} \equiv \xi R_{ij}$ , where  $R_{ij}$  contains the dependence on the initial and final quark masses (*cf.* Eq. (A.8)), and in the limit of a single heavy quark  $j = \{c\}$ , and three light flavors  $i = \{u, d, s\}$  in the initial state, it reduces to  $R_{ij} = (1 + m_c^2/Q^2)$ . In this case we recover the relation:  $\bar{\xi} = \xi (1 + m_c^2/Q^2)$  [25, 29, 57].

Note that Eqs. (36) and (37) lead to a generalized Callan–Gross relation at leading-order (with  $x$  replaced by  $\xi$ ):  $2\xi F_{1,l}^{\nu,(0)}(\xi) = F_{2,l}^{\nu,(0)}(\xi)$ . It is also important to note in Eqs. (39), (40), and (41) that operationally  $F_i^{\nu,(0)}$  is a function of the variable  $\xi$ , while the PDFs are functions of  $\bar{\xi} = \xi R_{ij}$ . As discussed in Appendix B, this is simply a consequence of evaluating the final state partonic momentum conserving delta-function  $\delta(\xi - \bar{\xi}/R_{ij})$ .

#### 4.2. Relation to TMC Structure Functions

From the master equation (21), we can relate the above partonic distributions to the TMC structure functions. The charm mass effects can be taken into account in the structure functions  $F_i^{\nu,(0)}$  in Eqs. (39)–(41) by using the generalized Nachtmann variable  $\bar{\xi}$ , thereby allowing the form of Eq. (21) to be kept unmodified. For example, in the limit of a diagonal CKM matrix,  $V_{ij} = \delta_{ij}$ , and neglecting the non-leading terms, inserting  $F_{2,c}^{\nu,(0)}(\xi, Q^2) \simeq 2\bar{\xi}s(\bar{\xi})$  into the leading term of Eq. (23) gives:

$$\begin{aligned} F_{2,c}^{\text{TMC}}(x, Q^2) &\simeq \frac{x^2}{\xi^2 r^3} F_{2,c}^{\nu,(0)}(\xi, Q^2) \simeq \frac{x^2}{\xi^2 r^3} 2\bar{\xi}s(\bar{\xi}) \\ &= \frac{2x^2}{r^3} (1 + m_c^2/Q^2)^2 \frac{s(\bar{\xi}, Q^2)}{\bar{\xi}}. \end{aligned} \quad (43)$$

The complete set of expressions in this “diagonal CKM” limit for the charm production component of the target mass corrected structure functions is given by:

$$\begin{aligned} F_{1,c}^{\text{TMC}}(x, Q^2) &\simeq \frac{x}{\bar{\xi}r} (1 + m_c^2/Q^2)s(\bar{\xi}) + \frac{2M^2 x^2}{Q^2 r^2} (1 + m_c^2/Q^2) \int_{\bar{\xi}}^1 du \frac{s(u)}{u}, \\ &\quad + \frac{4M^4 x^3}{Q^4 r^3} \int_{\bar{\xi}}^1 du \int_u^1 dv \frac{s(v)}{v}, \end{aligned} \quad (44)$$

$$\begin{aligned} F_{2,c}^{\text{TMC}}(x, Q^2) &\simeq \frac{2x^2}{\bar{\xi}r^3} (1 + m_c^2/Q^2)^2 s(\bar{\xi}) + \frac{12M^2 x^3}{Q^2 r^4} (1 + m_c^2/Q^2) \int_{\bar{\xi}}^1 du \frac{s(u)}{u} \\ &\quad + \frac{24M^4 x^4}{Q^4 r^5} \int_{\bar{\xi}}^1 du \int_u^1 dv \frac{s(v)}{v}, \end{aligned} \quad (45)$$

$$F_{3,c}^{\text{TMC}}(x, Q^2) \simeq \frac{x}{\bar{\xi}r^2} (1 + m_c^2/Q^2) 2s(\bar{\xi}) + \frac{2M^2 x^2}{Q^2 r^3} \int_{\bar{\xi}}^1 du \frac{2s(u)}{u} + 0. \quad (46)$$

A discussion of the dependence of  $h_i$  and  $g_2$  on the charm quark mass is given in Appendix B. \*

Having illustrated the implementation for non-zero hadron and quark masses, the extension to the general mass case is straightforward from the relations in Appendix B.

\* See also Ref. [42], Eqs. (3.1)–(3.3); with  $g_2$  and  $h_3$  defined as in Eqs. (B.4) and (B.5), the charm mass dependent structure functions of Eqs. (44)–(46) are recovered.

As with the above charm mass case, the form of the equations will remain the same; the target mass dependence enters in the replacement  $x \rightarrow \xi = xR_M$ , where  $R_M = 2/(1+r)$  (see Appendix A), and the quark masses enter via the replacement  $\xi \rightarrow \bar{\xi} = \xi R_{ij}$ .

## 5. Threshold Effects and the $x \rightarrow 1$ Limit

The standard TMC formulation described in the previous sections involves the so-called “threshold problem”, which was recognized soon after the original derivation of TMCs, and has been discussed by a number of authors in the literature [39, 58–61]. It is associated with the behavior of parton distributions in the threshold region, between pion-production ( $W = M + m_\pi$ ) and the elastic point ( $W = M$ ), and becomes increasingly important as  $x \rightarrow 1$ .

The problem can be summarized as follows. For simplicity, we neglect perturbative QCD (pQCD) corrections, with the Wilson coefficient functions  $C_i^n$  set to unity. Following Ref. [34], we define a leading twist parton distribution in this discussion by  $F(\xi, Q^2) \equiv F_2^{(0)}(\xi, Q^2)/\xi^2$  (*cf.* Eq. (12)). The  $n$ -th moment of the parton distribution,

$$A_n = \int_0^1 d\xi \xi^n F(\xi, Q^2) , \quad (47)$$

should be  $Q^2$  independent. Neglecting higher twist (HT) contributions, one should have [39, 58]:

$$\int_0^1 d\xi \xi^{n-2} F_2^{(0)}(\xi, Q_1^2) = \int_0^1 d\xi \xi^{n-2} F_2^{(0)}(\xi, Q_2^2) \quad [\text{no pQCD, no HT}] \quad (48)$$

for any two momentum scales  $Q_1^2$  and  $Q_2^2$ , where  $F_2^{(0)}(\xi, Q^2)$  is the structure function in the massless target limit,  $M \rightarrow 0$  (see Eq. (25)). Since  $F_2^{(0)}(\xi, Q^2)$  must vanish in the kinematically forbidden region  $\xi > \xi_0$ , where

$$\xi_0(Q^2) \equiv \xi(x=1, Q^2) = 2/(1 + \sqrt{1 + 4M^2/Q^2}) , \quad (49)$$

the equality in Eq. (48) implies that  $F_2^{(0)}(\xi, Q^2)$  must be zero for both  $\xi > \xi_0(Q_1^2)$  and  $\xi > \xi_0(Q_2^2)$ . If  $Q_1^2 < Q_2^2$ , in which case  $\xi_0(Q_1^2) < \xi_0(Q_2^2)$ , this implies that  $F_2^{(0)}(\xi, Q_2^2)$  must vanish in the range  $\xi_0(Q_1^2) < \xi < \xi_0(Q_2^2)$ . However, there is no physical reason in the parton model for it to do so here, and this leads to an unphysical constraint.

According to the prescription of De Rújula, Georgi and Politzer (DGP) [39], the solution to this “paradox” lies in the higher order terms in the twist expansion for the moments of  $F_2^{(0)}(\xi, Q^2)$ . In general, the  $n$ -th moment of the structure function  $F_2^{(0)}(\xi, Q^2)$  can be written as [39] (*cf.* Eq. (34))

$$\int_0^1 d\xi \xi^{n-2} F_2^{(0)}(\xi, Q^2) = A_n + \sum_{i=1}^{\infty} \left( \frac{nM_0^2}{Q^2} \right)^i B_{n,i} , \quad (50)$$

where the  $i$ -th term in the sum is the contribution of operators of twist  $2i+2$ .

DGP argue [39] that the higher twist  $B_{n,i}$  terms indeed tame the paradox. They note that if the distribution at large  $\xi$  behaves as  $(1-\xi)^a$ , with  $a \approx 3-4$ , then the  $n$ -th moment of  $F_2^{(0)}$  will be sensitive to the distribution at values of  $\xi$  close to

$\xi_n \equiv n/(n+a) \approx 1 - a/n$  for large  $n$ . For the moments to be sensitive to the threshold region, one must take  $n$  large enough so that  $\xi_n \approx \xi_0(Q^2) \approx 1 - M^2/Q^2$  at large  $Q^2$ . In other words, the analysis is affected strongly by the region in moment space where  $n \approx aQ^2/M^2$ . For such large values of  $n$ , however, the terms proportional to  $B_{n,i}$  cannot be disregarded, and DGP conclude that there is therefore no paradox.

More specifically, there is a non-uniformity in the limits  $n \rightarrow \infty$  (or  $\xi \rightarrow 1$ ) and  $Q^2 \rightarrow \infty$ . The appearance of powers of  $nM_0^2/Q^2$  in Eq. (50) signals the breakdown of the whole twist expansion in this region. The master equation (21) is therefore not valid for large  $\xi$ , where higher twists are important.

The problem with the nonuniform limits was also recognized by Tung and collaborators [59, 60], in the context of Nachtmann moments, which were discussed in Sec. 2. In particular, they pointed out that the Nachtmann moments  $\mu_i^n(Q^2)$  of structure functions have, for fixed  $n$ , the asymptotic  $Q^2 \rightarrow \infty$  limit (again, neglecting pQCD corrections)

$$\mu_i^n(Q^2) \rightarrow A_n \quad [n \text{ fixed}, Q^2 \rightarrow \infty, \text{ no pQCD}] . \quad (51)$$

However, the asymptotic form does not exhibit the correct threshold behavior at fixed  $Q^2$ , which should be [59, 60]

$$\mu_i^n(Q^2) \rightarrow \xi_0^n(Q^2) \tilde{\mu}_i^n(Q^2) \quad [Q^2 \text{ fixed}, n \rightarrow \infty] , \quad (52)$$

where  $\tilde{\mu}_i^n(Q^2)$  are the “regularized” moments of a function which has support over the correct physical range,  $0 < \xi < \xi_0$ . In the asymptotic  $n \rightarrow \infty$  limit, the regularized moments are then weakly dependent upon  $n$ , while the full moments  $\mu_i^n$  contain the main  $n$  dependence through the threshold factor  $\xi_0^n(Q^2)$  [59, 60].

Tung *et al.* [59, 60] proposed a solution to this problem by postulating an *ansatz* for the moments in which the threshold factor is explicitly included in the definition,

$$\mu_i^{n \text{ (Tung)}}(Q^2) \equiv \xi_0^n(Q^2) A_n , \quad (53)$$

where the new moments are consistent with both the asymptotic QCD behavior (51) and the kinematic threshold requirement (52). However, as they note, such a prescription is not unique, and in fact agrees with the standard OPE expansion only in the  $n \rightarrow \infty$  limit [61].

The region of  $Q^2$  where TMCs are significant also corresponds to the region where nucleon resonances play an important role,  $W \lesssim 2$  GeV. Although the resonance region displays significant  $Q^2$  dependent structure, a twist expansion is still useful here when one averages over individual resonances. The resonance region corresponds to  $n \lesssim aQ^2/M^2$ , and here higher twists are small but not negligible. The size of the higher twists in fact determines the degree to which the physical structure function oscillates around the leading twist function, in the sense of local Bloom–Gilman duality [11]. Target mass corrections are therefore closely related to the physics of resonances and quark–hadron duality [12].

Duality is also invoked implicitly in the DGP approach in that the parton distribution in the region between the pion production threshold, corresponding to

$W = M + m_\pi$ , and  $\xi = 1$  is taken to be dual to the elastic form factor at  $\xi = \xi_0$  [11, 62, 63]. However, a consequence of a non-zero parton distribution  $F(\xi, Q^2)$  over the entire region  $0 \leq \xi \leq 1$ , including the unphysical region  $\xi > \xi_0$  (at  $x > 1$ ), is that the target mass corrected structure function is non-zero at  $x = 1$ , *i.e.*,  $F_2^{\text{TMC}}(x = 1, Q^2) > 0$ , for any finite  $Q^2$ . This seems necessary in the DGP approach if one wishes to preserve a probabilistic interpretation for  $F(\xi)$ , as in the parton model.

An alternative to working with distributions in the unphysical region  $\xi > \xi_0$  was suggested by Steffens and Melnitchouk (SM) in Ref. [61]. The philosophy adopted there was to reformulate the DGP analysis in such a way as to ensure the correct kinematic limit for the target mass corrected structure function, *i.e.*,  $F_2^{\text{TMC}}(x \rightarrow 1, Q^2) \rightarrow 0$ , for any finite  $Q^2$ . The method specifically involved working with parton distributions which vanish beyond the kinematic upper limit,  $\xi = \xi_0$ , and which at finite  $Q^2$  therefore depend on  $\xi$  and  $\xi_0$ .

The approach of SM [61] defines the matrix element  $A_n^{(\text{SM})}$  in terms of an integral of the parton distribution over the range  $0 \leq \xi \leq \xi_0$ ,

$$A_n^{(\text{SM})} \equiv \int_0^{\xi_0} d\xi \xi^n F(\xi, \xi_0), \quad (54)$$

where the function  $F$  is now  $\xi$  and  $\xi_0$  dependent, and vanishes smoothly as  $\xi \rightarrow \xi_0$ , for instance as a power of  $(\xi_0 - \xi)$ . The function  $F$  is also properly normalized; for example, if the functional form for  $F$  is  $F(\xi, \xi_0) = N \xi^a (\xi_0 - \xi)^b$ , then the normalization constant is  $N = \xi_0^{-a-b-1}$ .

One can also define a “scaled Nachtmann variable”

$$\tilde{\xi} = \frac{\xi}{\xi_0}, \quad (55)$$

and write  $A_n^{(\text{SM})}$  in a form resembling that in DGP,

$$A_n^{(\text{SM})} = \xi_0^n \int_0^1 d\tilde{\xi} \tilde{\xi}^n \tilde{F}(\tilde{\xi}), \quad (56)$$

where now the function  $\tilde{F}$  depends *only* on a single variable  $\tilde{\xi}$ . In this approach, one does not need to invoke higher twists to cancel the leading twist TMCs in the  $\xi > \xi_0$  region. In the original DGP formulation, the extended, unphysical range  $\xi > \xi_0$  implies that the target mass corrected structure function is overestimated at large  $\xi$ . A resulting complication of this is that even neglecting pQCD, the moments  $A_n^{(\text{SM})}$  become  $Q^2$  dependent, thereby making the connection with the OPE, and hence a partonic interpretation, problematic in the presence of TMCs. This  $Q^2$  dependence is, however, in accordance with the results of Tung *et al.*, Eq. (53).

An alternative approach to avoid introducing this additional  $Q^2$  dependence is to redefine the moments such that

$$A_n^{(\text{SM}') \equiv} \int_0^{\xi_0} d\xi \left(\frac{\xi}{\xi_0}\right)^n F(\xi, \xi_0). \quad (57)$$

In terms of the variable  $\tilde{\xi}$  this can then be rewritten as

$$A_n^{(\text{SM}') \equiv} \int_0^1 d\tilde{\xi} \tilde{\xi}^n \tilde{F}(\tilde{\xi}). \quad (58)$$

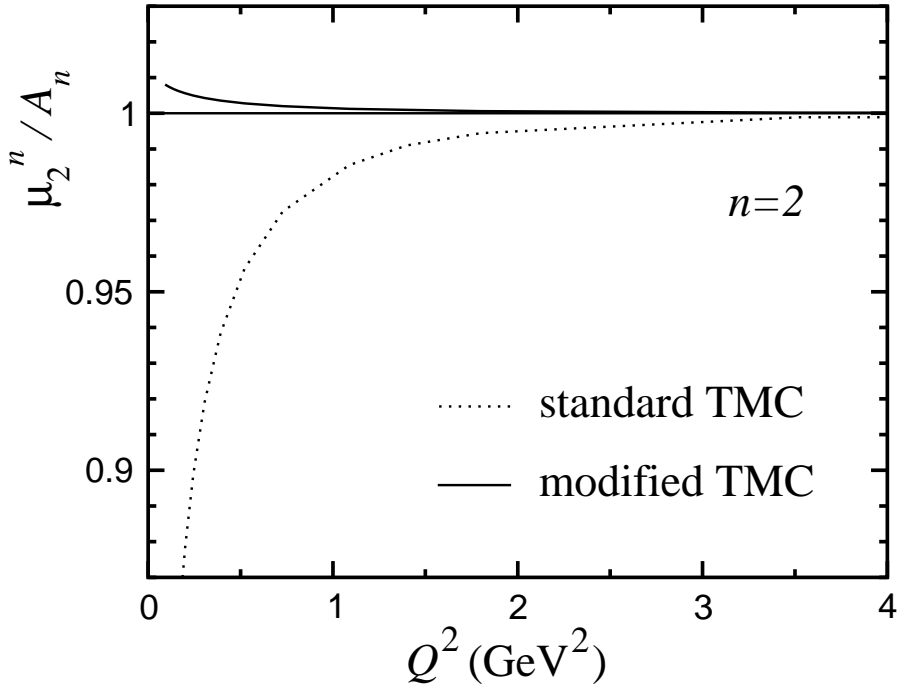


**Figure 6.** Ratio of the  $n = 2$  Nachtmann moment of the  $F_2$  structure function and the  $n = 2$  moment of the quark distribution, as a function of  $Q^2$ . The curves correspond to standard TMC prescription [34] (dotted) and the modified TMC (SM) prescription from Ref. [61].

This definition leads to the standard approach of Georgi & Politzer,  $A_n^{(\text{SM}')} \rightarrow A_n$ , with the unphysical region contributing in the calculation of the physical structure functions. Hence, we arrive at a conundrum: imposing the correct threshold leads to a  $Q^2$  dependent  $A_n$ , in contradiction to the standard OPE; retaining the partonic interpretation of  $A_n$  gives rise, on the other hand, to unphysical contributions to the physical structure functions, which one hopes will be canceled by higher twists.

The large- $x$  behavior of the distributions is also particularly important for the comparison of the Nachtmann moments  $\mu_i^n$  of structure functions with the moments of the parton distributions. The Nachtmann moments are, by construction, meant to be protected from target mass effects, so that these should be equal to the moments of the scaling parton distributions for *any*  $Q^2$ . A comparison of the Nachtmann moment with  $A_n$  was already shown in Fig. 3, and in Ref. [61] this property was investigated in several other scenarios including the modified definition of the parton distribution in Eq. (56).

In the standard approach, Eq. (58), there is an increasing difference between the Nachtmann moments and the moments of the parton distributions for  $Q^2 < 1 \text{ GeV}^2$ , as can be seen in the ratio shown in Fig. 6. At  $Q^2 = 1 \text{ GeV}^2$ , the difference is  $\approx 2\%$ .

In the modified approach, on the other hand (Eq. (56)), the Nachtmann moments are essentially equivalent to the  $\xi_0$ -dependent  $A_n^{(\text{SM})}$  for  $Q^2$  as low as  $0.5 \text{ GeV}^2$ , as shown with the solid line.

The deviation of the “standard TMC” ratio from unity below  $Q^2 \sim 2 - 3 \text{ GeV}^2$  suggests that the equality between the Cornwall–Norton moments of the PDFs (or massless limit structure functions) and the Nachtmann moments of the target mass corrected structure functions will only hold at sufficiently large  $Q^2$ . For  $Q^2 \gtrsim 2 \text{ GeV}^2$ , we can expect uncertainties due to the treatment of TMCs to be  $\lesssim 1\%$ . These effects will also appear when the evaluations are done using experimental data. For lower values of  $Q^2$ , the direct connection between Nachtmann moments of  $F_2^{\text{TMC}}$  and the parton model requires a more sophisticated treatment of the large- $x$  regime.

## 6. Quantitative Effects of Target Mass Corrections

The target mass corrections described in the previous sections, and summarized in the master equations (21), are applied in this section to neutrino–nucleon and electron–proton scattering. The theoretical evaluation of the target mass corrected structure functions  $F_2$  and  $F_3$  are compared with data from the NuTeV neutrino–iron scattering experiment [64]. (In this discussion we neglect nuclear effects on structure functions, and assume equality between the nuclear and nucleon structure functions — for a discussion of nuclear effects in inclusive lepton–nuclear scattering, see *e.g.* Ref. [65].) We also show results for the electromagnetic structure function  $F_2^p$  in electron–proton scattering, with a comparison data. We begin in Sec. 6.1. with the ratio of  $F_2$  and  $F_3$  evaluated in  $\nu N$  scattering ( $N = (p + n)/2$ ) with and without target mass corrections.

### 6.1. TMC Effects in the Massless Quark Limit

Target mass corrections are relevant especially in the high- $x$  and low- $Q^2$  regions. To quantify the size of the corrections, we evaluate the structure functions at leading order in QCD, for neutrino–nucleon scattering in the massless quark limit. For convenience we use the CTEQ5 PDF set [6]; using other parameterizations has a minimal effect on our numerical results. The effects of the target mass corrections are illustrated in Fig. 7, where the ratios of the  $F_2$  and  $F_3$  structure functions with and without TMC effects are shown, namely  $F_i^{\text{TMC}}/F_i^{(0)}$ ,  $i = 2, 3$ , for  $Q^2 = 1, 5, 25$  and  $125 \text{ GeV}^2$ .

The ratios of structure functions with TMCs to those without rise above unity at large  $x$ , with the rise beginning at larger values of  $x$  as  $Q^2$  increases. The correction can be quite large: for  $x = 0.8$ , for example, the TMC effect is  $\sim 30\%$  at  $Q^2 = 5 \text{ GeV}^2$ . A large part of the correction comes from the shift of  $x \rightarrow \xi < x$  in the PDFs. The PDFs are rapidly falling functions at large  $x$ , so even a small change in the argument of the PDFs ( $x$  replaced by  $\xi$ ) can have a significant impact on  $F_i^{\text{TMC}}/F_i^{(0)}$ . For  $Q^2 = 1 \text{ GeV}^2$ ,  $\xi$  deviates from  $x$  even for  $x \sim 0.3$  (see Fig. 2). In the following section we discuss the relative importance of the non-leading terms in the master equations (21).

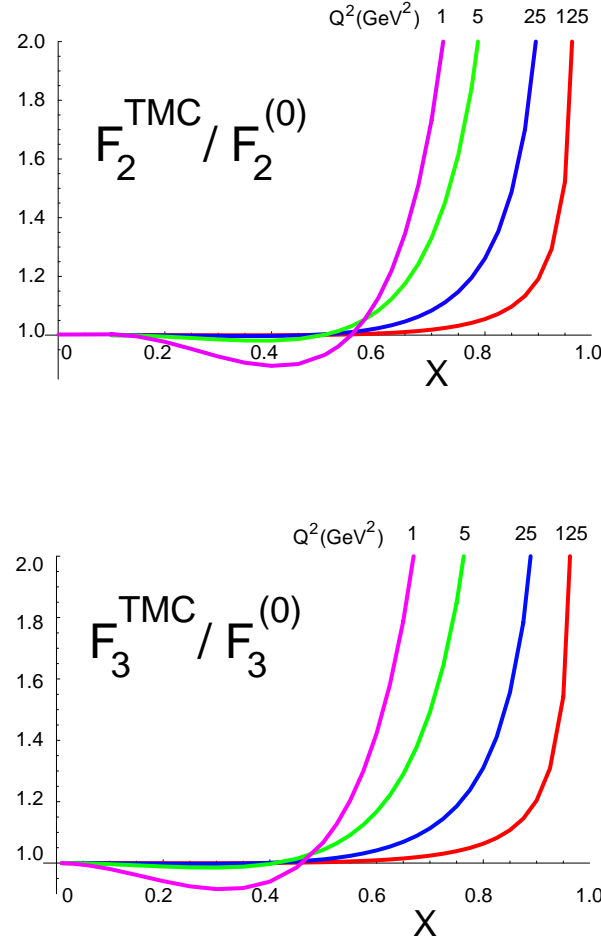


**Figure 7.** Ratio of the  $F_2$  and  $F_3$  structure functions with and without target mass corrections ( $F_i^{\text{TMC}} / F_i^{(0)}$ ,  $i = 2, 3$ ) vs.  $x$  for  $Q^2 = \{1, 5, 25, 125\} \text{ GeV}^2$ .

## 6.2. Non-leading Terms in the Master Equations

The non-leading (second and third) terms in Eqs. (22)–(24) constitute a small correction to the leading term. Since the evaluation of the convolution integrals is quite time-consuming, it is useful to have an upper bound for the size of these terms. We can rewrite Eq. (23) as:

$$F_2^{\text{TMC}}(x, Q^2) = \frac{x^2}{\xi^2 r^3} F_2^{(0)}(\xi) \left[ 1 + \frac{6\mu x}{r} \frac{\xi^2 h_2(\xi)}{F_2^{(0)}(\xi)} + \frac{12\mu^2 x^2}{r^2} \frac{\xi^2 g_2(\xi)}{F_2^{(0)}(\xi)} \right]$$

with  $\mu = M^2/Q^2$ . The structure function  $F_2^{(0)}$  appearing in the integrals in Eqs. (18) and (20) is a decreasing function of  $x$  or  $\xi$  (see *e.g.* Fig. 10 below). Consequently,  $F_2^{(0)}$  can be evaluated at the lower integral limit, giving  $h_2(\xi) < (F_2^{(0)}(\xi)/\xi)(1 - \xi)$  and  $g_2(\xi) < F_2^{(0)}(\xi)(-\ln \xi - 1 + \xi)$ . One then arrives at the following inequality:

$$F_2^{\text{TMC}}(x, Q^2) < \frac{x^2}{\xi^2 r^3} F_2^{(0)}(\xi) \left[ 1 + \frac{6\mu x \xi}{r} (1 - \xi) + \frac{12\mu^2 x^2 \xi^2}{r^2} (-\ln \xi - 1 + \xi) \right]. \quad (59)$$

The expressions  $(6\mu x\xi/r)(1-\xi)$  and  $(12\mu^2 x^2 \xi^2/r^2)(-\ln \xi - 1 + \xi)$  can be easily evaluated to obtain an upper bound for the contribution of the non-leading terms. Following the same line of argumentation one finds for the structure function  $F_3$ :

$$F_3^{\text{TMC}}(x, Q^2) < \frac{x}{\xi r^2} F_3^{(0)}(\xi) \left[ 1 - \frac{2\mu x \xi}{r} \ln \xi \right]. \quad (60)$$

While the upper bounds for  $F_2^{\text{TMC}}$  and  $F_3^{\text{TMC}}$  are strictly satisfied for  $x$  and  $Q^2$  values relevant for target mass corrections, these bounds are of limited practical use. For example, for  $Q^2 = 1 \text{ GeV}^2$ , Eq. (59) places a limit on the non-leading corrections to be less than  $\sim 65\%$  of the leading term at large  $x$ . The actual value is much less, below  $\sim 21\%$ . Therefore it is useful to note that

$$F_2^{\text{TMC}}(x, Q^2) \simeq \frac{x^2}{\xi^2 r^3} F_2^{(0)}(\xi) \left[ 1 + \frac{6\mu x \xi}{r} (1 - \xi)^2 \right] \quad (61)$$

provides a very good approximation of the structure function  $F_2^{\text{TMC}}(x, Q^2)$ . Similarly,  $F_3^{\text{TMC}}(x, Q^2)$  can be approximated by

$$F_3^{\text{TMC}}(x, Q^2) \simeq \frac{x}{\xi r^2} F_3^{(0)}(\xi) \left[ 1 - \frac{\mu x \xi}{r} (1 - \xi) \ln \xi \right]. \quad (62)$$

The magnitude of the non-leading contributions to the target mass correction is illustrated in Fig. 8, where the ratio of the target mass corrected  $F_2$  (top graph) and  $F_3$  (bottom graph) structure functions is shown relative to the leading contribution, at  $Q^2 = 1, 4$  and  $10 \text{ GeV}^2$ . Here  $F_2^{\text{TMC,leading}}(x, Q^2) = (x^2/\xi^2 r^3) F_2^{(0)}(\xi)$  represents the leading contribution to the target mass corrected structure function  $F_2^{\text{TMC}}(x, Q^2)$  (*cf.* Eq. (23)), while the corresponding results for the  $F_3$  structure function is given by  $F_3^{\text{TMC,leading}}(x, Q^2) = (x/\xi r^2) F_3^{(0)}(\xi)$ . For definiteness, the structure functions are for charged current neutrino–proton scattering and have been computed in next-to-leading order of QCD including quark mass effects. However, the results are very robust concerning variations of these details (process, order, quark mass effects). The dotted curves in Fig. 8 present the results of the approximate formulas in Eqs. (61) and (62). As can be seen, the simple approximations are in very good agreement with the exact results.

The excess over unity depicts the fractional contribution of the non-leading terms. Clearly, the non-leading contributions to the structure function  $F_2^{\text{TMC}}$  are relatively small and positive. For  $Q^2 = 1 \text{ GeV}^2$  they amount about 21%. However, for  $Q^2 = 4 \text{ GeV}^2$  they correct the leading term already by less than 6%, and for  $Q^2 = 10 \text{ GeV}^2$  by less than 3%. The major contribution from the non-leading pieces comes from the terms proportional to  $h_2$  or  $h_3$ , whereas the part proportional to  $g_2$  constitutes a small correction. These results imply that  $F_2^{\text{TMC}}(x, Q^2)$  can be approximated in many cases by  $F_2^{\text{TMC,leading}}(x, Q^2)$ . Moreover, if more precision is needed, the non-leading pieces can be simulated, to good accuracy, by the simple approximation in Eq. (61). For  $F_3^{\text{TMC}}$ , the non-leading terms are even smaller, contributing less than 7% for  $Q^2 = 1 \text{ GeV}^2$ . For  $Q^2 = 4 \text{ GeV}^2$  they are already below the 2% level.

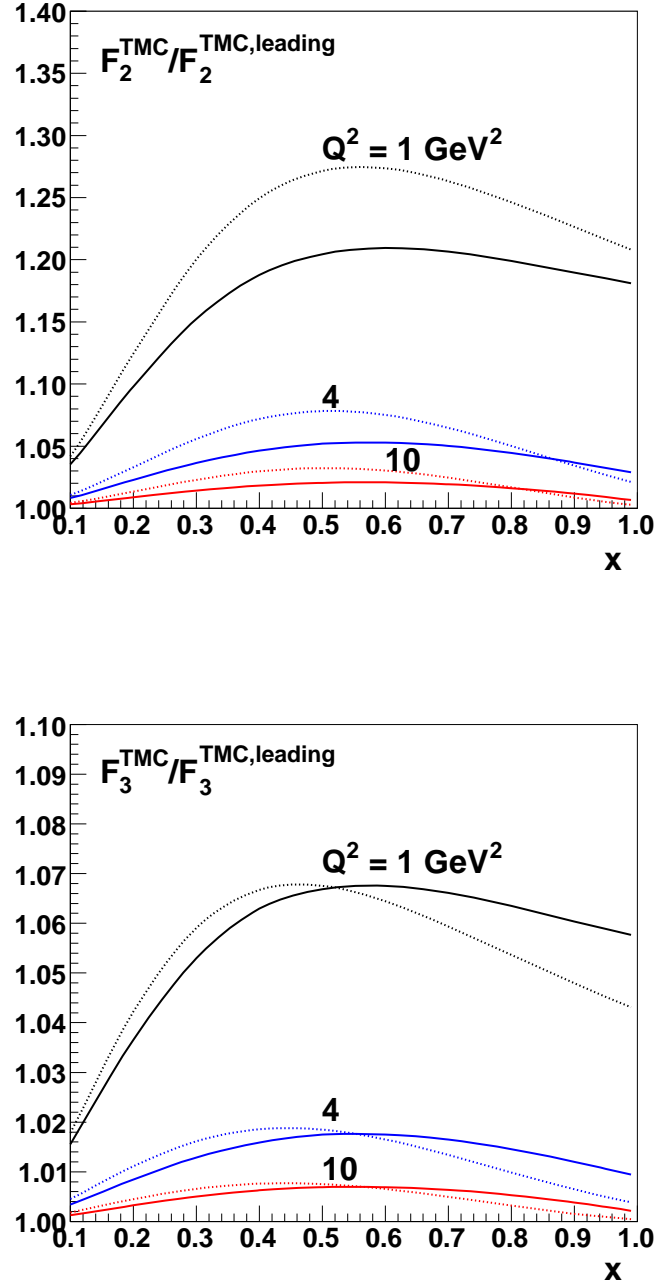


**Figure 8.** Ratio of the target mass corrected  $F_2^{\text{TMC}}(x, Q^2)$  (top) and  $F_3^{\text{TMC}}(x, Q^2)$  (bottom) structure functions to the leading contributions in Eqs. (23) and (24), at  $Q^2 = 1, 4$  and  $10 \text{ GeV}^2$ . The solid curves represent the exact results, while the dotted curves have been calculated using the approximate formulas in Eqs. (61) and (62).

The findings of this section are useful in providing a simple explanation of the main effects of the target mass corrections shown in Fig. 7. In fact, to good accuracy, the

ratio in Fig. 7 is given by:

$$\frac{F_2^{\text{TMC}}(x)}{F_2^{(0)}(x)} \simeq \frac{x^2}{\xi^2 r^3} \frac{F_2^{(0)}(\xi)}{F_2^{(0)}(x)}. \quad (63)$$

Since  $\xi < x$ , and  $F_2$  is a monotonically decreasing function, one can see that the simple shift from  $x$  to  $\xi$  in the argument of  $F_2^{(0)}$  (along with the factor  $x^2/\xi^2 > 1$ ) produces the enhancement over unity visible in this figure. The dip below unity for low  $Q^2$  values and intermediate  $x$  can be explained by the factor  $1/r^3$  in Eq. (63) which is smaller than one.

### 6.3. TMC Effects in NuTeV Structure Functions

A comparison of the  $F_2$  structure function with the NuTeV neutrino data [64] is shown in Fig. 9, where  $F_2$  is calculated both with (solid curves) and without (dashed curves) target mass corrections. For this comparison, the full NLO evaluation is made including charm quark mass effects. The PDF set for this comparison was taken to be CTEQ6HQ [7]. As Fig. 9 shows, there is a clear improvement in the agreement in the high- $x$  region between the NuTeV data and NLO predictions including target mass effects.

### 6.4. Unfolding Target Mass Effects From Structure Function Data

In neutrino and charged lepton scattering from nucleons it is the  $F_i^{\text{TMC}}(x, Q^2)$  functions that are measured by experiment. In principle, measurements over a range in  $x$  at fixed  $Q^2$  allow for a determination of the massless limit structure functions  $F_i^{(0)}(x)$  by inverting the master equations of Sec. 2. Implicit in such a procedure is the assumption that dynamical higher twists operators either contribute negligibly to the data in the region of interest, or that they also obey the master equations for the TMCs. Under such conditions the unfolding procedure then allows both the  $F_i^{(0)}(x)$  and the target mass contributions to be determined directly from data. The procedure is to parameterize  $F_i^{(0)}(x)$  at fixed  $Q^2$ , insert this into the master equations, and then minimize the difference of the resulting  $F_i^{\text{TMC}}$  with respect to the data.

This method is complementary to PDF fits. One might expect the  $F_2^{(0)}$  structure function so extracted to be consistent with that obtained from PDF fits to the data when including TMCs. However, an advantage of the unfolding procedure is that the separation of the  $F_2^{(0)}$  (which is described by pQCD) from the target mass contributions is good to all orders in  $\alpha_s$ , since Eq. (23) is valid to all orders. Comparisons of the results from the two techniques could help resolve any possible mixing between contributions from TMCs, higher twists, and those from higher order pQCD terms. Such an unfolding procedure has been undertaken [66] for the world data set of charged lepton scattering data from the proton, and the results are currently being prepared for publication.

In this study the  $F_2$  data were fitted globally for  $0.5 < Q^2 < 250$  GeV $^2$  by allowing for a  $Q^2$  dependence of the parameters describing  $F_2^{(0)}(x)$ . The results for  $Q^2 = 3$  (top panel) and 20 GeV $^2$  (bottom panel) are shown in Fig. 10. The solid curve

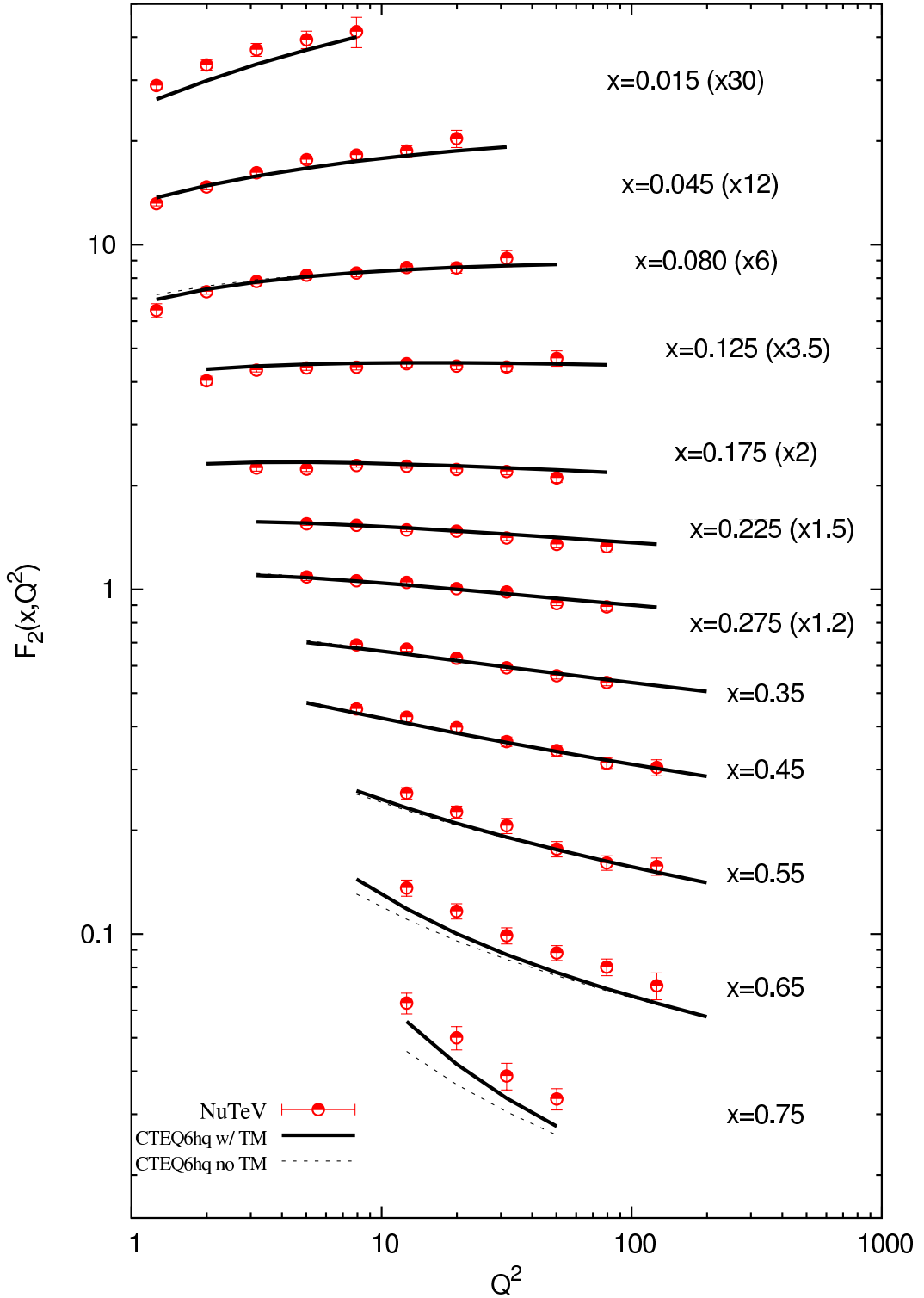


**Figure 9.** Comparison of the  $F_2$  structure function, with and without target mass corrections, and NuTeV data [64]. The base PDF set is CTEQ6HQ [7].

is the  $F_2^{(0)}$  determine from the fit, while the dashed curve is the full  $F_2^{\text{TMC}}$ . Consistent with the determination from PDF fits previously discussed, the TMC contributions to

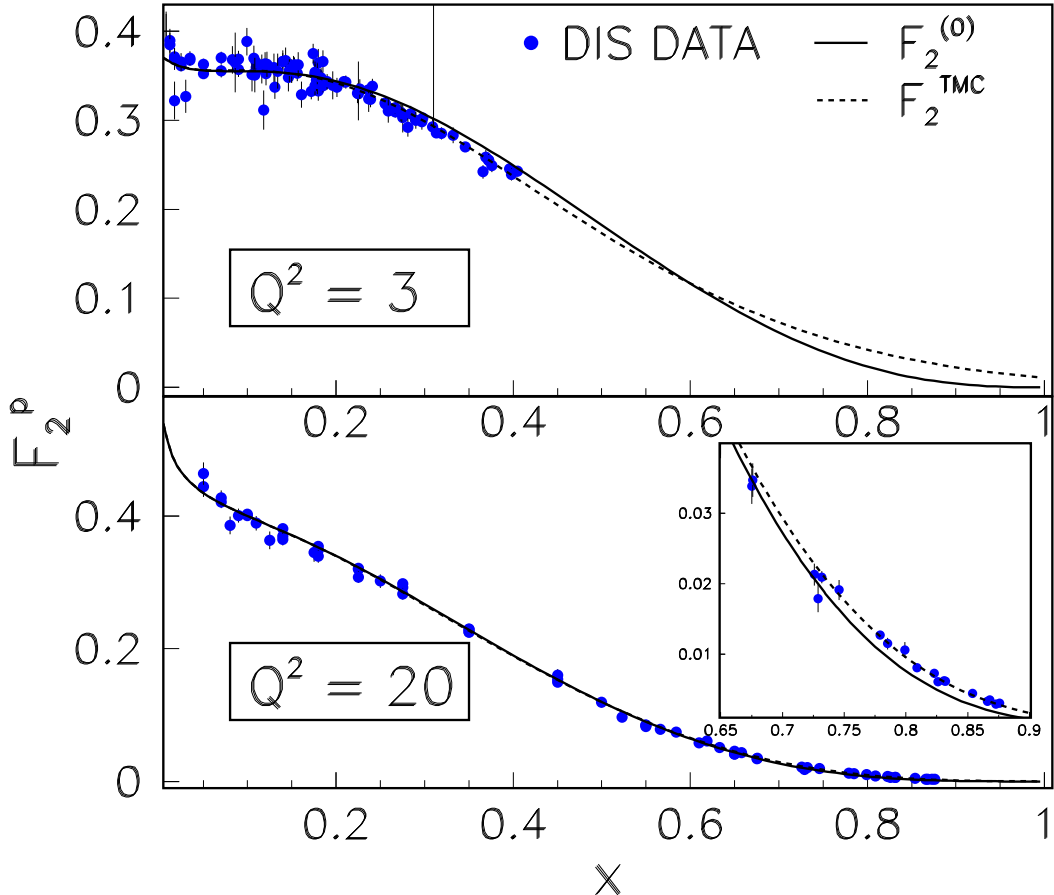


**Figure 10.** Results of the unfolding procedure of Ref. [66] for the proton  $F_2^p$  structure function, at  $Q^2 = 3 \text{ GeV}^2$  (top panel) and  $Q^2 = 20 \text{ GeV}^2$  (bottom panel). The massless limit functions are shown by the solid curves, and the target mass corrected results by the dashed curves.

$F_2$  are large at small  $Q^2$ , as much as 9% even at  $x = 0.4$  for  $Q^2 = 3 \text{ GeV}^2$ . While the TMCs become much smaller at higher  $Q^2$ , they are still sizable at higher  $x$ , as can be seen in the inset in Fig. 10 (bottom panel). At  $Q^2 = 20 \text{ GeV}^2$  the contributions from TMCs are 4%, 8% and 14% at  $x = 0.65, 0.70$  and  $0.75$ , respectively.

It is interesting to note that even in kinematic regions where the TMCs are large, the unfolding procedure gives results for the target mass contributions which are quite consistent with that determined by inserting existing CTEQ6 PDFs into the master equation for  $F_2$ . This can be observed in Fig. 11, where the ratio of TMC factors determined from the unfolding procedure to those calculated from CTEQ6 PDFs are plotted. The correction factors are here defined as  $F_2^{(0)} / F_2^{\text{TMC}}$ , e.g. the multiplicative factor which would be applied to data to yield a measured  $F_2^{(0)}$ . Figure 11 shows the

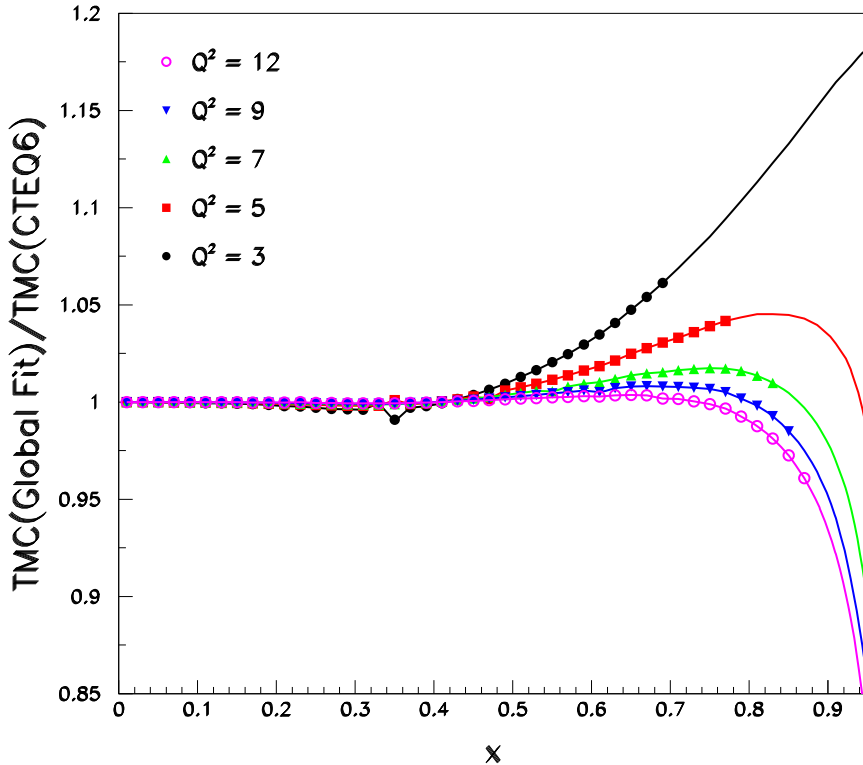


**Figure 11.** Ratio of target mass corrections for  $F_2^p$  determined from the unfolding procedure (global fit) of Ref. [66] to the corrections obtained from CTEQ6 PDFs *cf.* Eq. (64). The  $Q^2$  values shown are in  $\text{GeV}^2$ . The  $x$  region for which  $W^2 > 4 \text{ GeV}^2$  is indicated by the symbols. Note that even at high  $x$  and low  $Q^2$  the difference in the TMCs is typically less than several percent.

double ratio

$$\frac{\left(F_2^{(0)} / F_2^{\text{TMC}}\right)_{\text{unfold}}}{\left(F_2^{(0)} / F_2^{\text{TMC}}\right)_{\text{CTEQ6}}} \quad (64)$$

as a function of  $x$  for  $3 < Q^2 < 9 \text{ GeV}^2$ . For the region  $W^2 > 4 \text{ GeV}^2$  (indicated by the symbols) the difference is typically less than a few percent even up to  $x \approx 0.9$ .

As a final note, the size of the non-leading terms from the unfolding procedure is shown in Fig. 12 as a function of  $x$  for  $Q^2$  in the range 1 to  $12 \text{ GeV}^2$ . We display the ratio of the full  $F_2^{\text{TMC}}$  to that including only the leading term (top panel), and next-to-leading term (bottom panel); note the change of scale between the two panels. The fractional contribution from the leading term is found to be in excellent agreement to that shown in Fig. 8, while the contribution from the double integral term is at most 1.5% at  $Q^2 = 1 \text{ GeV}^2$ , and negligible for higher  $Q^2$ .

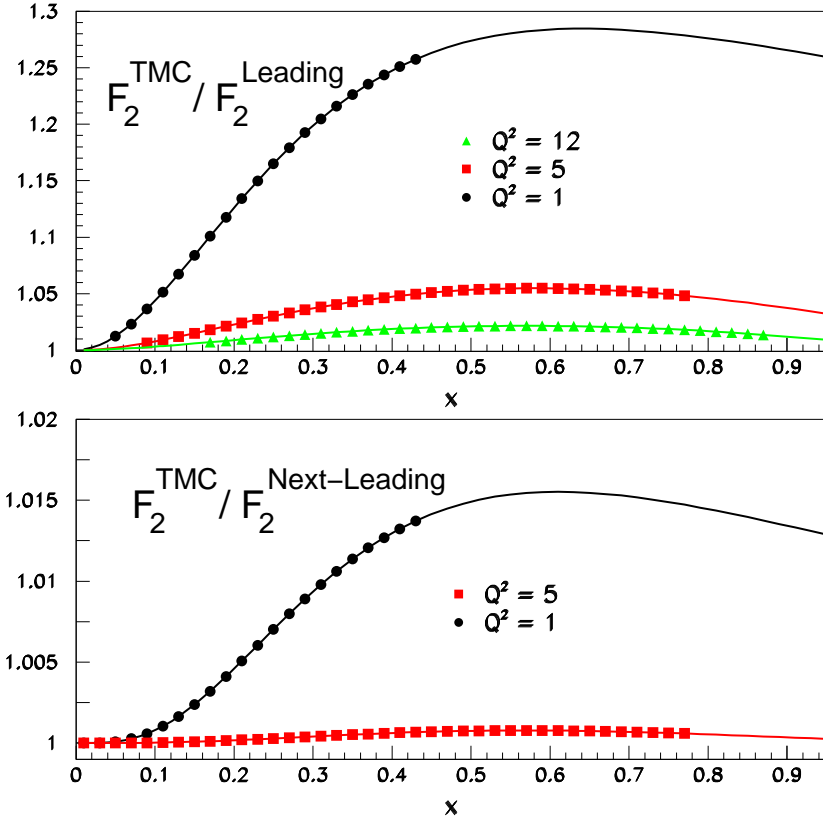


**Figure 12.** Ratio of the full  $F_2^{\text{TMC}}$ , as extracted from the unfolding procedure, to that including only the leading term  $F_2^{\text{TMC},\text{Leading}}$  (top panel), and next-to-leading term  $F_2^{\text{TMC},\text{Next-Leading}}$  (bottom panel), for  $Q^2 = \{1, 5, 12\}$   $\text{GeV}^2$ . The  $x$  region for which  $W^2 > 4 \text{ GeV}^2$  is indicated by the symbols. Note the change of scale between the two panels.

### 6.5. Longitudinal Structure Function

Finally, we show a set of plots for the longitudinal structure function,  $F_L$ , in Fig. 13. The target mass corrected structure function  $F_L^{\text{TMC}}(x, Q^2)$  has been computed according to Eq. (26) using parton model results for the structure function  $F_L^{(0)}(x, Q^2)$  for charged current neutrino–proton scattering in NLO QCD including quark mass effects. Because the massless leading-order parton model contributions to  $F_L^{(0)}$  vanish, this quantity is ideally suited to study both mass effects and higher order corrections.

The effects of the TMC are illustrated in Figure 13a) where the ratio  $F_L^{(0)}/F_L^{\text{TMC}}$  is shown for  $Q^2 = 1, 4, 10$ , and  $20 \text{ GeV}^2$ . Note that the present ratio is the inverse of similar ratios shown in Fig. 7 for the structure functions  $F_2$  and  $F_3$ . As can be seen, the curves are steeply falling, implying very large target mass corrections. While the TMC are proportionately large in this region, unfortunately the longitudinal structure function becomes vanishingly small. This point is evident in Fig. 13b) where we plot the absolute magnitude of  $F_L$ . Here, the solid lines represent the full target mass corrected  $F_L^{\text{TMC}}(x, Q^2)$ , and the dashed lines represent the conventional parton model  $F_L^{(0)}(x, Q^2)$ .

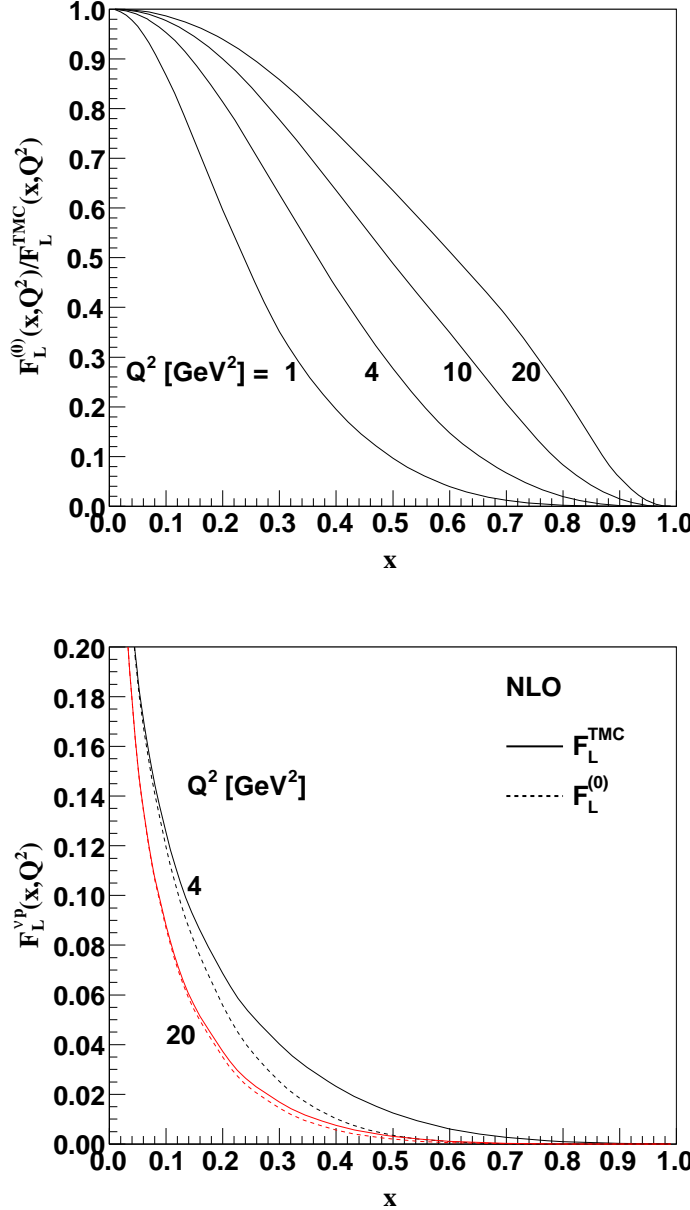


**Figure 13.** a) Ratio of the structure function  $F_L$  without ( $F_L^{(0)}(x, Q^2)$ ) and with ( $F_L^{\text{TMC}}(x, Q^2)$ ) target mass corrections at  $Q^2 = 1, 4, 10$ , and  $20 \text{ GeV}^2$  vs.  $x$  b) Absolute magnitude of the target mass corrected  $F_L^{\text{TMC}}(x, Q^2)$  (solid) as compared with the structure function in the limit of a vanishing target mass  $F_L^{(0)}(x, Q^2)$  (dashed) at  $Q^2 = 4$  and  $20 \text{ GeV}^2$  vs.  $x$ .

We do observe for  $Q^2 = 4 \text{ GeV}^2$  that there are significant differences in the intermediate  $x$  region ( $\sim 0.3$ ); however, these effects are negligible for  $Q^2 = 20 \text{ GeV}^2$ . In conclusion, we note that while the longitudinal structure function,  $F_L$ , is difficult to measure because

of its small size, a precise measurement of this quantity could prove to be sensitive to the TMC and quark mass effects.[67]

## 7. Conclusions

We have presented in this review a survey of the key issues pertaining to target mass corrections (TMCs) in inclusive lepton–nuclear scattering structure functions and their impact on the analysis of experimental results. As illustrated by our structure function results with and without TMC terms (Figs. 9–12), current experimental accuracy demands that these effects be properly incorporated.

In the context of the operator product expansion (OPE), we have outlined the derivation of the master equation for the target mass corrected structure functions  $F_j^{\text{TMC}}(x, Q^2)$ , Eq. (21), without any assumptions about fixed-order perturbation theory or the Callan–Gross relation. However, when relating the OPE results to calculable parton model expressions, we are forced to make compromises; for example, we generally work with only at leading twist (*cf.* Sec. 3) and at a finite order of  $\alpha_s$  in perturbation theory. Because the TMCs enter as  $(M^2/Q^2)^j$  corrections, it is essential to organize our expansion so that these terms can be distinguished from true higher twist contributions, such as from four-quark operators.

To illustrate the dependence on both hadron and parton masses in the formalism, we present explicit results for heavy quark production via neutrino–nucleon scattering. For the non-leading terms, we compute an upper limit for the integral terms, derive approximate expressions, and evaluate the full expression numerically; as expected, the dominant TMC effects arise at large  $x$  and small  $Q^2$  values.

In the limit  $x \rightarrow 1$  we encounter an additional complication in the standard TMC formulation, associated with the non-vanishing of the target mass corrected structure function at  $x = 1$ . This problem arises if the massless limit structure function,  $F_2^{(0)}(\xi, Q^2)$ , is not required to vanish in the kinematically forbidden region  $\xi > \xi_0$ . One may hope that higher twist terms could cancel the unphysical contributions. Alternatively, one can enforce the constraint that  $F_2^{(0)}(\xi, Q^2)$  does vanish for  $\xi > \xi_0$ , which removes the unphysical contributions, but at the expense of introducing additional  $\xi_0$  dependence into the structure function. We have reviewed various attempts that have been made in the literature to address this problem.

Finally, the importance of the TMCs for comparison with experimental data is established in Sec. 6. We perform fits of structure functions both with and without the TMC contributions, and observe that these terms can have a substantive impact in the region of high  $x$ . While there are a number of factors which enter these fits, it is encouraging to see that the TMC contributions generally improve the agreement between the fits and data.

We also demonstrate (Figs. 10, 11, and 12) quantitative agreement extracting the  $F_2$  structure function with two complementary methods. We find that the ratio of the TMCs for  $F_2$  obtained starting with PDFs and including TMCs, *vs.* starting with the

TMC master equation, agrees at the 5% or better level, even for  $Q^2 = 3 \text{ GeV}^2$  for  $x < 0.65$ .

The fact that the experimental data are sufficiently accurate to be sensitive to the TMC effects represents an important milestone in the study of inelastic lepton–nucleon scattering. From this foundation, future studies can more fully characterize the TMC effects, and begin to separately identify higher twist contributions for these processes.

## Acknowledgments

We thank Stefan Kretzer, Jorge Morfin, Joseph (Jeff) Owens, A. Kataev, Ingo Sick, for valuable discussions. F.I.O., I.S., and J.Y.Y. acknowledge the hospitality of Argonne, BNL, CERN, and Fermilab where a portion of this work was performed. This work was partially supported by the U.S. Department of Energy under grant DE-FG02-04ER41299, DE-FG02-91ER40685, DE-FG02-91ER40664, DE-FG03-95ER40908, contract W-31-109-ENG-38; contract DE-AC05-06OR23177 (under which Jefferson Science Associates LLC operates the Thomas Jefferson National Accelerator Facility), the National Science Foundation grant 0400332, the Lightner-Sams Foundation, and the Sam Taylor Foundation. The work of J. Y. Yu was supported by the Deutsche Forschungsgemeinschaft (DFG) through grant No. YU 118/1-1.

## Appendix A.

### Kinematics and Fundamental Relations

#### *Appendix A.1.*

##### *Notation*

We consider the basic inclusive lepton–nuclear scattering process  $\ell(k) + N(P) \rightarrow \ell'(k') + X(P_X)$  (*cf.* Fig. 1), with  $q = k - k'$  the four-momentum transferred to the nucleon, and define  $x$  to be the standard DIS scaling variable in the Bjorken limit:

$$x = \frac{-q^2}{2P \cdot q} = \frac{Q^2}{2M\nu} , \quad (\text{A.1})$$

where  $-Q^2 = q^2$  is the virtuality of the exchanged boson, and  $P$  is the target hadron four-momentum, with  $M$  the target nucleon mass ( $P^2 = M^2$ ). We denote by  $m_i$  the mass of the  $i$ 'th quark. For a nuclear target with atomic number  $A$ , it is convenient to rescale the Bjorken variable  $x$  by  $A$  so that the denominator of Eq. (A.1) is still the mass of a nucleon. Additionally, we introduce the energy transferred to the hadronic system in the target rest frame as:

$$\nu = E - E' = \frac{P \cdot q}{M} \quad (\text{A.2})$$

and the inelasticity

$$y = \frac{E - E'}{E} = \frac{P \cdot q}{P \cdot k} , \quad (\text{A.3})$$

where  $E$  and  $E'$  represent the initial and final lepton energies, respectively. The mass of the hadronic final state is given by:

$$W^2 = P_X^2 = (P + q)^2 = M^2 + \frac{Q^2}{x}(1 - x) . \quad (\text{A.4})$$

For convenience, we also introduce the variable  $r$ , which is a combination of factors that appears frequently:

$$r = \sqrt{1 + \frac{4x^2 M^2}{Q^2}} \equiv \sqrt{1 + \frac{Q^2}{\nu^2}} .$$

### Appendix A.2.

#### Generalized Nachtmann Variable

For massless quarks, the parton light-cone fraction is given by the Nachtmann variable  $\xi$ . Given the 4-vector  $P_\mu = \{P_t, P_x, P_y, P_z\}$ , we can re-express this in light-cone coordinates as  $P_\mu = \{P_+, \vec{P}_\perp, P_-\}$  where<sup>#</sup>  $P_\pm = (P_t \pm P_z)/\sqrt{2}$  and  $\vec{P}_\perp = \{P_x, P_y\}$  are the (boost-invariant) transverse components. Light-cone coordinates are a convenient representation when the momentum components are strongly ordered, *e.g.*  $P_+ \gg P_\perp, P_-$ . Thus, if the hadron light-cone vector is  $P_\mu = \{P^+, \vec{0}, M^2/(2P^+)\}$ , the parton vector for a (massless) parton is  $p_\mu = \{\xi P^+, \vec{0}, 0\}$ .<sup>††</sup> In the case of massive partons, the Nachtmann variable  $\xi$  is generalized to  $\bar{\xi}$ . [29, 57, 68]

We identify two generalized Nachtmann-type of variables,  $\xi$  and  $\bar{\xi}$ , which are related to the Bjorken  $x$  variable via a dimensionless multiplicative factor. These can be written as:

$$\xi = x R_M , \quad (\text{A.5})$$

$$\bar{\xi} = \xi R_{ij} = x R_M R_{ij} , \quad (\text{A.6})$$

where

$$R_M = \frac{2}{1 + \sqrt{1 + (4x^2 M^2/Q^2)}} = \frac{2}{1 + r} , \quad (\text{A.7})$$

$$R_{ij} = \frac{Q^2 - m_i^2 + m_j^2 + \Delta(-Q^2, m_i^2, m_j^2)}{2Q^2} , \quad (\text{A.8})$$

$$\Delta(a, b, c) = \sqrt{a^2 + b^2 + c^2 - 2(ab + bc + ca)} , \quad (\text{A.9})$$

where  $m_i$  is the initial quark mass and  $m_j$  is the final quark mass. The variable  $\xi = x R_M$  essentially corrects Bjorken  $x$  for the effects of the hadronic mass. Computationally, this arises from the final state momentum conserving delta-function,  $\delta^4(q + P - P_X)$ , which can be re-expressed to include the delta-function  $\delta(x - \xi/R_M)$ .

In a similar manner, the variable  $\bar{\xi} = \xi R_{ij}$  further corrects the  $\xi$  variable for the effects of the partonic masses. The origin of this correction is the momentum conserving

<sup>#</sup> There are multiple conventions here; sometimes the  $1/\sqrt{2}$  is replaced by a  $1/2$  or a  $1$ .

<sup>††</sup>The parton model is derived in the collinear limit where the parton transverse momentum is neglected, *e.g.*  $\vec{p}_\perp = 0$ ; finite transverse momentum can contribute to the TMCs, *cf.* Sec. 1.

delta-function at the partonic level,  $\delta^4(q + p_i - p_j)$ , which can be re-expressed to include  $\delta(\xi - \bar{\xi}/R_{ij})$ .

It is important to note that the hadronic correction  $R_M$  and the partonic mass corrections  $R_{ij}$  are separate and can be applied multiplicatively. Also note that the  $R_{ij}$  correction factor depends on the specific partonic masses involved; hence, this cannot be simply factored out as with the  $R_M$  terms.

In the limit the initial quark mass vanishes ( $m_i \rightarrow 0$ ), the partonic correction factor has the limit  $R_{ij} \rightarrow (1 + m_j^2/Q^2)$ , which we recognize as the original slow-rescaling correction:

$$\bar{\xi} = \xi(1 + m_j^2/Q^2), \quad m_i = 0.$$

Our focus in including quark mass corrections is for charm production in neutrino scattering, where incident quark masses are negligible, or where heavy quark PDFs are very small and additionally suppressed by small mixing angles. Consequently we shall focus on the  $m_i = 0$  results below.

## Appendix B.

### Charm Mass Dependence in $h_2$ and $g_2$

We discuss here the charm mass,  $m_c$ , dependence in the target mass corrected structure functions in Eqs. (44)–(46). Inserting  $F_2^{(0)}$  from Eq. (40) into the definition of  $h_2(\xi)$  in Eq. (18), we find (for a diagonal CKM matrix):

$$h_2(\xi) \equiv \int_{\xi}^1 du \frac{F_2^{(0)}(u)}{u^2} = \int_{\xi}^1 du \frac{2\bar{u}s(\bar{u})}{u^2} = 2(1 + m_c^2/Q^2) \int_{\xi}^1 du \frac{s(\bar{u})}{u}, \quad (\text{B.1})$$

where the variable  $\bar{u} = u(1 + m_c^2/Q^2)$ . Making a variable transformation to  $\bar{u}$ , we find:

$$h_2(\xi) = 2(1 + m_c^2/Q^2) \int_{\xi}^1 du \frac{s(\bar{u})}{u} = 2(1 + m_c^2/Q^2) \int_{\bar{\xi}}^{1+m_c^2/Q^2} d\bar{u} \frac{s(\bar{u})}{\bar{u}}. \quad (\text{B.2})$$

Since the strange quark PDF vanishes for  $\bar{u} > 1$  we can restrict the upper integration bound to 1 and arrive at the final result:

$$h_2(\xi) = 2(1 + m_c^2/Q^2) \int_{\bar{\xi}}^1 du \frac{s(u)}{u}. \quad (\text{B.3})$$

Similar steps lead to the results:

$$g_2(\xi) = 2 \int_{\bar{\xi}}^1 du \int_u^1 dv \frac{s(v)}{v}, \quad (\text{B.4})$$

$$h_3(\xi) = \int_{\bar{\xi}}^1 du \frac{2s(u)}{u}. \quad (\text{B.5})$$

## Appendix C.

### Comparisons with the Literature

In this appendix, we make the identification of our notation with the notation in earlier papers by Georgi & Politzer [34], De Rújula, Georgi & Politzer [40], and Barbieri *et al.* [35]. We also comment on the relation to the notation of the paper by Kretzer & Reno [42]. Known typographic errors are also indicated in this appendix, in an attempt to minimize confusion when comparing results in the literature. Since neutrino production of charm quarks has both target mass and charm quark corrections, we make the comparison for charm production in the diagonal Cabibbo matrix limit.

#### Appendix C.1.

##### Comparisons with Georgi & Politzer

The results for the target mass corrected structure functions in the work of Georgi & Politzer [34] are given in their Eqs. (4.19), (4.20) and (4.22). Only leading order in QCD is considered, which in the massless limit yields the Callan–Gross relation for the  $F_1$  and  $F_2$  structure functions. As a result, a function  $F(\xi)$  is the only function introduced. Before proceeding, we should correct two typographic errors in Ref. [34]:

- (i) In relation (4.19) of Ref. [34]:

$$W_1(Q^2, x) = \frac{x}{2(1 + 4M^2/Q^2)^{1/2}} F(\xi) + \dots \rightarrow \frac{x}{2(1 + 4x^2 M^2/Q^2)^{1/2}} F(\xi) \quad (\text{C.1})$$

- (ii) In relation (4.22) of Ref. [34]: No derivation of  $W_3$  is provided to get the overall factor, but there is a factor 2 mismatch in relative normalization between the first and second terms:

$$\frac{\nu W_3(Q^2, x)}{M} = \frac{x}{2(1 + 4x^2 M^2/Q^2)} F(\xi) + \dots \rightarrow \frac{x}{(1 + 4x^2 M^2/Q^2)} F(\xi) \quad (\text{C.2})$$

With these corrections, Eqs. (4.19) and (4.20) of Ref. [34] agree with Eqs. (22) and (23) at leading order if  $F(\xi)$  in [34] is identified with the structure functions  $F_i^{(0)}(\xi)$  such that:

$$F(\xi) = F_2^{(0)}(\xi)/\xi^2 = 2F_1^{(0)}(\xi)/\xi. \quad (\text{C.3})$$

Note that  $F_2^{(0)}(\xi)/\xi^2 = 2F_1^{(0)}(\xi)/\xi$  is the Callan–Gross relation which holds in leading order for massless quarks.

The target mass corrected structure function  $\nu W_3/M$  found in Eq. (4.22) in Ref. [34], after correcting the typographic error, agrees with Eq. (24) if:

$$F_3 = \frac{\nu}{2M} W_3 \quad \text{and} \quad F(\xi) = 2F_3^{(0)}(\xi)/\xi. \quad (\text{C.4})$$

In Ref. [40] De Rújula *et al.* discuss the electromagnetic structure functions, where  $F(\xi) \rightarrow F_1^S(\xi)$  or  $F_2^S(\xi)$ . The  $F_i^S$  are not defined, however, in terms of the structure

functions  $F_i^{(0)}$ . In addition, the structure functions  $W_1$  and  $W_2$  are a factor of  $1/M$  times the  $W_i$  defined in Ref. [34].

### Appendix C.2.

#### Comparisons with Barbieri, Ellis, Gaillard, & Ross

In comparing with the notation of Barbieri, Ellis, Gaillard, & Ross [35], we note firstly that the quantity “ $\nu$ ” in [35] is scaled by a factor  $M$  compared to our notation, and we label it with a subscript  $\nu_B$ :

$$\nu_B = \nu M , \quad (\text{C.5})$$

which gives  $x = Q^2/(2\nu_B) = Q^2/(2M\nu)$ . Note also that the variable denoted by “ $\xi$ ” in Ref. [35] corresponds to the generalized Nachtmann variable  $\bar{\xi}$  used in this paper.

Substituting our notation in Eqs. (2.12a–e) of Ref. [35] yields:

$$W_1^B = (a^2 + b^2) \frac{x}{r} \left[ \left( 1 + \frac{m_f^2 + m_i^2}{Q^2} \right) \mathcal{F}_i^B(\bar{\xi}) + \mathcal{G}_i^B \right] - (a^2 - b^2) \frac{2x m_i m_f}{Q^2 r} \mathcal{F}_i^B(\bar{\xi}) , \quad (\text{C.6})$$

$$W_2^B = (a^2 + b^2) \frac{4x^3 M^2}{r^3 Q^2} \left[ \left( \frac{R}{Q^2} \right)^2 \mathcal{F}_i^B(\bar{\xi}) + 3\mathcal{G}_i^B \right] , \quad (\text{C.7})$$

$$W_3^B = 2ab \frac{4x^2 M^2}{r^2 Q^2} \left[ \left( \frac{R}{Q^2} \right)^2 \mathcal{F}_i^B(\bar{\xi}) + \frac{2x M^2}{r Q^2} \int_{\bar{\xi}}^1 du \left( 1 - \frac{m_i^2}{M^2 u^2} \right) \mathcal{F}_i^B(u) \right] . \quad (\text{C.8})$$

Here  $R^2 = [(Q^2 + m_f^2 - m_i^2)^2 + 4m_i^2 Q^2]$ ,  $m_i$  and  $m_f$  are the initial and final quark masses, and  $a$  and  $b$  are the vector and axial-vector couplings, respectively. The structure function  $\mathcal{F}_i$  corresponds to our  $F_i^{(0)}$ , and the  $\mathcal{G}_i$  term contains the single and double integral terms corresponding to our  $h_i$  and  $g_2$  expressions of Eq. (21).

With  $m_i^2 \ll m_f^2$ , in the first two structure functions

$$(a^2 + b^2) \mathcal{F}_i^B(\bar{\xi}) = \frac{s(\bar{\xi})}{\bar{\xi}} \quad (\text{C.9})$$

yields  $W_1^B$  and  $W_2^B$  with the same normalization as in Eq. (10). In the third structure function, we find that:

$$2ab \mathcal{F}_i^B(\bar{\xi}) = \frac{s(\bar{\xi})}{\bar{\xi}} . \quad (\text{C.10})$$

We obtain agreement for the third structure function if  $\nu_B W_3^B = 2M^2 F_3^{\text{TMC}}$ .

We note, however, that we do not match the expressions for Barbieri *et al.* [35] in the limit of a finite initial quark mass ( $m_i \neq 0$ ). While the initial quark mass terms are small numerically, for completeness we comment on the relation of our results to this work.

The renormalization and factorization prescriptions allow certain freedoms in organizing the terms in the master equation; hence, the mass dependence need not be

unique. Our results are constructed to a) reduce to standard parton model expressions in various limiting cases (*e.g.*  $\{m_i, m_f, M\} \rightarrow 0$ ), and to b) maintain the simple structure of Eq. (21). Our formulation incorporating quark masses follows the factorization construction of Collins [69]. In particular, the  $\{A, B, C\}$  coefficients for our master formula, Eq. (21), are free of any quark mass terms; the  $m_i$  dependence is entirely contained in  $F_i^{(0)}$ .

Our expressions also satisfy the expected limiting cases. For example, in the limit  $M \rightarrow 0$  our expressions reduce to the general parton model result with finite  $\{m_i, m_f\}$  terms, by construction; this is in contrast to Eqs. (C.6)–(C.8).

In summary, our expressions of Eq. (21) follow the simple factorized structure of Ref. [69], and reduce to the standard parton model results in the limits of various vanishing masses. The numerical difference between this formulation and that of Ref. [35] is small.

### Appendix C.3.

#### Comparisons with Kretzer & Reno

In Kretzer and Reno [42], the notation has the slow rescaling variable including the charm quark mass written as  $\xi/\lambda$ , where  $\lambda = (1 + m_c^2/Q^2)^{-1}$ , so that  $\xi/\lambda = \bar{\xi}$ . The quantity  $\rho$  in [42] equals  $r$ , and  $\mu = M^2/Q^2$ . In the absence of charm mass corrections, the results of Ref. [42] are in full agreement with the equations in this paper.

The translation of the treatment of  $F_i^{\text{TMC}}$  in terms of  $F_i^{(0)}$  in Ref. [42] is not made explicitly when charm production is involved. Charm production is discussed in terms of  $\mathcal{F}_i \sim s$ . The expression for charm production in Eq. (3.27) of Ref. [42] is written as the sum of three terms times coefficients. The terms depend on  $\mathcal{F}_i$ ,  $\mathcal{H}_i$  and  $\mathcal{G}_2$ . The quantity  $\mathcal{F}_i(\xi)$  appearing in Eq. (3.27) should read  $\mathcal{F}_i(\bar{\xi})$ , with

$$\mathcal{F}_i(\bar{\xi}) = s(\bar{\xi}) \quad (\text{C.11})$$

at leading order. The functions  $\mathcal{H}_i$  and  $\mathcal{G}_2$  in Ref. [42] for charm production should also be functions of  $\bar{\xi}$  rather than  $\xi$ . In terms of  $g_2$  and  $h_i$  introduced here, one has:

$$h_2(\xi) = 2(1 + m_c^2/Q^2)\mathcal{H}_2(\bar{\xi}) , \quad (\text{C.12})$$

$$g_2(\xi) = 2\mathcal{G}_2(\bar{\xi}) , \quad (\text{C.13})$$

$$h_3(\xi) = 2\mathcal{H}_3(\bar{\xi}) . \quad (\text{C.14})$$

With these corrections, Eq. (3.27) in Ref. [42] is:

$$F_j^{\text{TMC}}(x, Q^2) \rightarrow \sum \alpha_j^i \mathcal{F}_i(\bar{\xi}, Q^2) + \beta_j^i \mathcal{H}_i(\bar{\xi}, Q^2) + \gamma_j \mathcal{G}_2(\bar{\xi}, Q^2) . \quad (\text{C.15})$$

The sum is from  $i = 1, \dots, 5$ , however, there is no mixing of the 4th and 5th terms in  $F_{1,2,3}^{\text{TMC}}$ . Tables IV and V with the coefficients  $\alpha_j^i$  and  $\beta_j^i$  are correct, however, there is an error in Table VI. The coefficients  $\gamma_i$  all have an extra power of  $\lambda$  in the denominator. Explicitly, the first two coefficients should read (with the translated notation):

$$\gamma_1 = \frac{4M^4 x^3}{Q^4 r^3} , \quad (\text{C.16})$$

$$\gamma_2 = \frac{24M^4x^4}{Q^4r^5} . \quad (\text{C.17})$$

In fact, Eq. (C.15) was used in the numerical work in Ref. [42]. The contributions of  $\gamma_1$  and  $\gamma_2$  are small, so the error in Table VI is not numerically significant.

## References

- [1] Richard E. Taylor. Deep inelastic scattering: The Early years. *Rev. Mod. Phys.*, 63:573–595, 1991. and references therein.
- [2] Henry W. Kendall. Deep inelastic scattering: Experiments on the proton and the observation. *Rev. Mod. Phys.*, 63:597–614, 1991. and references therein.
- [3] Jerome I. Friedman. Deep inelastic scattering: Comparisons with the quark model. *Rev. Mod. Phys.*, 63:615–629, 1991. and references therein.
- [4] R. Devenish and A. Cooper-Sarkar. Deep inelastic scattering. Oxford, UK: Univ. Pr. (2004) 403 p.
- [5] M. Glück, E. Reya, and A. Vogt. Dynamical parton distributions revisited. *Eur. Phys. J.*, C5:461–470, 1998, hep-ph/9806404.
- [6] H. L. Lai et al. Global QCD analysis of parton structure of the nucleon: CTEQ5 parton distributions. *Eur. Phys. J.*, C12:375–392, 2000, hep-ph/9903282.
- [7] S. Kretzer, H. L. Lai, F. I. Olness, and W. K. Tung. CTEQ6 parton distributions with heavy quark mass effects. *Phys. Rev.*, D69:114005, 2004, hep-ph/0307022.
- [8] Sergey Alekhin, Kirill Melnikov, and Frank Petriello. Fixed target Drell-Yan data and NNLO QCD fits of parton distribution functions. *Phys. Rev.*, D74:054033, 2006, hep-ph/0606237.
- [9] Johannes Blümlein, Helmut Böttcher, and Alberto Guffanti. Non-singlet QCD analysis of deep inelastic world data at  $O(\alpha_s^3)$ . *Nucl. Phys.*, B774:182–207, 2007, hep-ph/0607200.
- [10] A. D. Martin, W. J. Stirling, R. S. Thorne, and G. Watt. Update of Parton Distributions at NNLO. *Phys. Lett.*, B652:292–299, 2007, arXiv:0706.0459 [hep-ph].
- [11] Elliott D. Bloom and Frederick J. Gilman. Scaling, duality, and the behavior of resonances in inelastic electron–proton scattering. *Phys. Rev. Lett.*, 25:1140, 1970.
- [12] W. Melnitchouk, R. Ent, and C. Keppel. Quark-hadron duality in electron scattering. *Phys. Rept.*, 406:127–301, 2005, hep-ph/0501217.
- [13] Guido Altarelli, R. K. Ellis, and G. Martinelli. Large Perturbative Corrections to the Drell-Yan Process in QCD. *Nucl. Phys.*, B157:461, 1979.
- [14] W. Furmanski and R. Petronzio. Lepton–hadron processes beyond leading order in quantum chromodynamics. *Zeit. Phys.*, C11:293, 1982.
- [15] M. Glück, R. M. Godbole, and E. Reya. Heavy flavor production at high-energy  $ep$  colliders. *Z. Phys.*, C38:441, 1988.
- [16] M. Glück, S. Kretzer, and E. Reya. The Strange Sea Density and Charm Production in Deep Inelastic Charged Current Processes. *Phys. Lett.*, B380:171–176, 1996, hep-ph/9603304.
- [17] J. A. M. Vermaseren, A. Vogt, and S. Moch. The third-order QCD corrections to deep-inelastic scattering by photon exchange. *Nucl. Phys.*, B724:3–182, 2005, hep-ph/0504242.
- [18] S. Moch, J. A. M. Vermaseren, and A. Vogt. The longitudinal structure function at the third order. *Phys. Lett.*, B606:123–129, 2005, hep-ph/0411112.
- [19] A. Vogt, S. Moch, and J. A. M. Vermaseren. The three-loop splitting functions in QCD: The singlet case. *Nucl. Phys.*, B691:129–181, 2004, hep-ph/0404111.
- [20] S. Moch, J. A. M. Vermaseren, and A. Vogt. The three-loop splitting functions in QCD: The non-singlet case. *Nucl. Phys.*, B688:101–134, 2004, hep-ph/0403192.
- [21] E. B. Zijlstra and W. L. van Neerven. Order  $\alpha_s^2$  correction to the structure function  $F_3(x, Q^2)$  in deep inelastic neutrino–hadron scattering. *Phys. Lett.*, B297:377–384, 1992.
- [22] E. B. Zijlstra and W. L. van Neerven. Order  $\alpha_s^2$  QCD corrections to the deep inelastic proton structure functions  $F_2$  and  $F_L$ . *Nucl. Phys.*, B383:525–574, 1992.
- [23] K. P. O. Diener, S. Dittmaier, and W. Hollik. Electroweak higher-order effects and theoretical uncertainties in deep-inelastic neutrino scattering. *Phys. Rev.*, D72:093002, 2005, hep-ph/0509084.
- [24] A. D. Martin, R. G. Roberts, W. J. Stirling, and R. S. Thorne. Parton distributions incorporating QED contributions. *Eur. Phys. J.*, C39:155–161, 2005, hep-ph/0411040.

- [25] R. Michael Barnett. Evidence for new quarks and new currents. *Phys. Rev. Lett.*, 36:1163–1166, 1976.
- [26] Edward Witten. Heavy quark contributions to deep inelastic scattering. *Nucl. Phys.*, B104:445–476, 1976.
- [27] Thomas Gottschalk. Chromodynamic corrections to neutrino production of heavy quarks. *Phys. Rev.*, D23:56, 1981.
- [28] John C. Collins and Wu-Ki Tung. Calculating heavy quark distributions. *Nucl. Phys.*, B278:934, 1986.
- [29] M. A. G. Aivazis, John C. Collins, Fredrick I. Olness, and Wu-Ki Tung. Leptoproduction of heavy quarks. 2) A unified QCD formulation of charged and neutral current processes from fixed target to collider energies. *Phys. Rev.*, D50:3102–3118, 1994, hep-ph/9312319.
- [30] M. Buza, Y. Matiounine, J. Smith, and W. L. van Neerven. Charm electroproduction viewed in the variable-flavour number scheme versus fixed-order perturbation theory. *Eur. Phys. J.*, C1:301–320, 1998, hep-ph/9612398.
- [31] A. Chuvakin, J. Smith, and W. L. van Neerven. Comparison between variable flavor number schemes for charm quark electroproduction. *Phys. Rev.*, D61:096004, 2000, hep-ph/9910250.
- [32] S. Kretzer and I. Schienbein. Heavy quark initiated contributions to deep inelastic structure functions. *Phys. Rev.*, D58:094035, 1998, hep-ph/9805233.
- [33] Otto Nachtmann. Positivity constraints for anomalous dimensions. *Nucl. Phys.*, B63:237–247, 1973.
- [34] Howard Georgi and H. David Politzer. Freedom at moderate energies: Masses in color dynamics. *Phys. Rev.*, D14:1829, 1976.
- [35] Riccardo Barbieri, John R. Ellis, M. K. Gaillard, and Graham G. Ross. Mass corrections to scaling in deep inelastic processes. *Nucl. Phys.*, B117:50, 1976.
- [36] Riccardo Barbieri, John R. Ellis, Mary K. Gaillard, and Graham G. Ross. A quest for a wholly scaling variable. *Phys. Lett.*, B64:171, 1976.
- [37] R. K. Ellis, W. Furmanski, and R. Petronzio. Power corrections to the parton model in QCD. *Nucl. Phys.*, B207:1, 1982.
- [38] R. K. Ellis, W. Furmanski, and R. Petronzio. Unraveling higher twists. *Nucl. Phys.*, B212:29, 1983.
- [39] A. De Rujula, Howard Georgi, and H. David Politzer. Trouble with  $\xi$  scaling? *Phys. Rev.*, D15:2495, 1977.
- [40] Alvaro De Rujula, Howard Georgi, and H. David Politzer. Demythification of Electroproduction, Local Duality and Precocious Scaling. *Ann. Phys.*, 103:315, 1977.
- [41] S. Kretzer and M. H. Reno. Tau neutrino deep inelastic charged current interactions. *Phys. Rev.*, D66:113007, 2002, hep-ph/0208187.
- [42] S. Kretzer and M. H. Reno. Target mass corrections to electro-weak structure functions and perturbative neutrino cross sections. *Phys. Rev.*, D69:034002, 2004, hep-ph/0307023.
- [43] J. Blümlein and A. Tkabladze. Target mass corrections to the spin-dependent structure functions. *J. Phys.*, G25:1553–1554, 1999, hep-ph/9812331.
- [44] Johannes Blümlein and Avtandil Tkabladze. Target mass corrections for polarized structure functions and new sum rules. *Nucl. Phys.*, B553:427–464, 1999, hep-ph/9812478.
- [45] Johannes Blümlein, Bodo Geyer, and Dieter Robaschik. Target mass and finite momentum transfer corrections to unpolarized and polarized diffractive scatterin. *Nucl. Phys.*, B755:112–136, 2006, hep-ph/0605310.
- [46] J. L. Miramontes and J. Sanchez Guillen. Understanding higher twist: Operator approach to power corrections. *Z. Phys.*, C41:247, 1988.
- [47] A. L. Kataev, G. Parente, and A. V. Sidorov. Higher twists and  $\alpha_s(M_Z)$  extractions from the NNLO QCD analysis of the CCFR data for the  $xF_3$  structure function. *Nucl. Phys.*, B573:405–433, 2000, hep-ph/9905310.
- [48] A. L. Kataev, G. Parente, and A. V. Sidorov. Fixation of theoretical ambiguities in the improved

fits to  $xF_3$  CCFR data at the next-to-next-to-leading order and beyond. *Phys. Part. Nucl.*, 34:20–46, 2003, hep-ph/0106221.

- [49] A. L. Kataev. Renormalons at the boundaries between perturbative and non-perturbative QCD. *Mod. Phys. Lett.*, A20:2007–2022, 2005, hep-ph/0505230.
- [50] I. L. Solovtsov and D. V. Shirkov. The analytic approach in quantum chromodynamics. *Theor. Math. Phys.*, 120:1220–1244, 1999, hep-ph/9909305.
- [51] W. L. van Neerven and E. B. Zijlstra. Order  $\alpha_s^2$  contributions to the deep inelastic Wilson coefficient. *Phys. Lett.*, B272:127–133, 1991.
- [52] Xiang-Dong Ji and Peter Unrau. Parton–hadron duality: Resonances and higher twists. *Phys. Rev.*, D52:72–77, 1995, hep-ph/9408317.
- [53] Edward V. Shuryak and A. I. Vainshtein. Theory of Power Corrections to Deep Inelastic Scattering in Quantum Chromodynamics. 2.  $Q^4$  Effects: Polarized Target. *Nucl. Phys.*, B201:141, 1982.
- [54] E. Stein, P. Gornicki, L. Mankiewicz, and A. Schäfer. QCD sum rule calculation of twist four corrections to Bjorken and Ellis–Jaffe sum rules. *Phys. Lett.*, B353:107–113, 1995, hep-ph/9502323.
- [55] M. Osipenko et al. Higher twist analysis of the proton  $g_1$  structure function. *Phys. Lett.*, B609:259–264, 2005, hep-ph/0404195.
- [56] Z. E. Meziani et al. Higher twists and color polarizabilities in the neutron. *Phys. Lett.*, B613:148–153, 2005, hep-ph/0404066.
- [57] M. A. G. Aivazis, Frederick I. Olness, and Wu-Ki Tung. Leptoproduction of heavy quarks. 1) General formalism and kinematics of charged current and neutral current production processes. *Phys. Rev.*, D50:3085–3101, 1994, hep-ph/9312318.
- [58] D. J. Gross, S. B. Treiman, and Frank A. Wilczek. Mass corrections in deep inelastic scattering. *Phys. Rev.*, D15:2486, 1977.
- [59] Khalil Bitar, Porter W. Johnson, and Wu-Ki Tung. QCD asymptotics and kinematic thresholds in deep inelastic scattering. *Phys. Lett.*, B83:114, 1979.
- [60] P. W. Johnson and Wu-Ki Tung. Structure functions and their moments as testing ground for QCD: The pandora’s box of mass effects. Contribution to Neutrino ’79, Bergen, Norway, June 18–22, 1979.
- [61] F. M. Steffens and W. Melnitchouk. Target mass corrections revisited. *Phys. Rev.*, C73:055202, 2006, nucl-th/0603014.
- [62] W. Melnitchouk. Local duality predictions for  $x \sim 1$  structure functions. *Phys. Rev. Lett.*, 86:35–38, 2001, hep-ph/0106073.
- [63] F. M. Steffens and K. Tsushima. Local duality and charge symmetry violation in quark distributions. *Phys. Rev.*, D70:094040, 2004, hep-ph/0408018.
- [64] M. Tzanov et al. Precise measurement of neutrino and anti-neutrino differential cross sections. *Phys. Rev.*, D74:012008, 2006, hep-ex/0509010.
- [65] S. A. Kulagin and R. Petti. Global study of nuclear structure functions. *Nucl. Phys.*, A765:126–187, 2006, hep-ph/0412425.
- [66] M. Eric Christy. Unfolding of target mass effects from structure function data. In preparation.
- [67] Y. Liang et al. Measurement of  $r = \sigma(l)/\sigma(t)$  and the separated longitudinal and transverse structure functions in the nucleon resonance region. 2004, nucl-ex/0410027.
- [68] Fredrick I. Olness and Wu-Ki Tung. Factorization of helicity amplitudes and angular correlations for electroweak processes. *Phys. Rev.*, D35:833, 1987.
- [69] John C. Collins. Hard-scattering factorization with heavy quarks: A general treatment. *Phys. Rev.*, D58:094002, 1998, hep-ph/9806259.